From the holdings of the Department of Special Collections , Princeton University Library, Princeton, NJ

These documents are either in the public domain, or can only be used for educational and research purposes (Fair use) as per U.S. Copyright law (text below). By accessing this file, all users agree that their use falls in the public domain or within fair use as defined by the copyrightlaw. We do not charge any permission or usage fees for the publication of images of material inour collections, including those provided by Princeton University Library, via our website, catalog, or directly from staff.For more information regarding copyright, credit, and citation please review the information onthe Copyright, Credit and Citation Guidelines page of our website.
https://library.princeton.edu/special-collections/policies/copyright-credit-and-citation-guidelines. If you have any questions, including how to order higher-quality images from the collection, contact Special Collections Public Services via our Ask Us! Form. https://library.princeton.edu/special-collections/ask-us

---

Doctoral Dissertations, 2011-2026 Psychology

2012

Electrogenic Dendrites of the Deep Cerebellar Nuclei

Schneider, Eve Rebecca

Princeton, NJ : Princeton University

---

http://arks.princeton.edu/ark:/88435/dsp011g05fb640

U.S. Copyright law: The copyright law of the United States (Title 17, §108, United States Code) governs the making of photocopies or other reproductions of copyrighted material. Under certain conditions specified in the law, libraries and archives are authorized to furnish a photocopy or other reproduction. One of these specified conditions is that the photocopy or reproduction is not to be used for any purpose other than private study, scholarship, or research. If a user makes a request for, or later uses, a photocopy or reproduction for purposes in excess of fair use that user may be liable for copyright infringement. This institution reserves the right to refuse to accept a copying order if, in its judgment, fulfillment of the order would involve a violation of copyright law. https://www.copyright.gov/title17/title17.pdf

ELECTROGENIC DENDRITES OF THE DEEP CEREBELLAR NUCLEI

Eve Rebecca Schneider

A DISSERTATION PRESENTED TO THE FACULTY OF PRINCETON UNIVERSITY IN CANDIDACY FOR THE DEGREE OF DOCTOR OF PHILOSOPHY

RECOMMENDED FOR ACCEPTANCE BY THE DEPARTMENT OF PSYCHOLOGY

Advisor: Samuel S.-H. Wang

November 2012

© Copyright by Eve Rebecca Schneider, 2012. All rights reserved.

Abstract

The purpose of this thesis is to investigate whether neurons of the deep cerebellar nuclei (DCN) have active dendrites. DCN neurons are the critical output of the cerebellum, essential to all behaviors in which the cerebellum is involved and necessary for the consolidation of learning in the cerebellum. Despite their importance in the cerebellar circuit our understanding of the biophysical properties of these neurons is scant. Early work hints at the possibility that deep nuclear neurons might have active dendrites. If dendrites were capable of local amplification of synaptic input, they would provide a stage of integration prior to the neuron's spike output, and also provide a means by which plasticity could be determined by events occurring near the location of synapses. Experiments contained in this thesis demonstrate for the first time that DCN neurons exhibit three of the hallmarks of active dendrites found elsewhere in the central nervous system (CNS). First, they produce large dendritic calcium spikes comparable in amplitude to dendritic action potentials in other CNS neurons. Second, dendritic calcium signals do not diminish with distance from the soma, as would be expected for passive backpropagation. Third, DCN dendrites can generate calcium signals even in the presence of tetrodotoxin, a sodium channel blocker that abolishes action potential firing in vertebrate neurons. Instead, DCN calcium transients require the action of T-type calcium current, a voltage-gated conductance found in many other excitable dendrite types. Together these results suggest that DCN neurons have active dendrites capable of processing separate from the soma. Finally, the ability of DCN dendrites to generate calcium spikes is considerably enhanced by the addition of phorbol-12-myristate-13-acetate, an activator of the G protein-coupled receptor target protein kinase C (PKC). Thus the excitability of DCN dendrites may be increased under the influence of

neuromodulators, which are known to regulate attention, learning, and a host of other systems-level functions.

Acknowledgements

So many people have provided help and support during this PhD that it is hard to fully express my gratitude in a page. I would especially like to acknowledge my advisor, Samuel S.-H. Wang, and my thesis committee for all their efforts.

I am deeply indebted to all my former PIs up to and during grad school: George Wagner, Bartley Hoebel, Samuel S.H. Wang, and Shaun Jordan. Alan Gelperin and David Tank provided crucial scientific advice and mentoring, and their practical neuroscience course was an incredible resource. Likewise, thanks to Stephan Thiberge and Peter Rickgauer for their help with optics. David Linden provided advice on the use of phorbol esters. And of course, thanks to Tom Otis for hosting me at UCLA and giving me another crack at the climbing fiber collateral synapse!

There are a number of people who have been invaluable for stimulating discussions, experimental tips, moral support and general camaraderie. These are the people who remind one another that science is important! Tyson Aflalo, Dimitriy Aronov, Aleksandra Badura, Patrick Bradley, Bernd Kuhn, Chandramouli Chandrasekaran, Charles Burlingame, Damian Carrieri, Forrest Colman, Nikhil Desmuk, Cristina Domnisoru, Andrew Fink, Andrea Giovannuci, Amy Gleichman, Andrea Granstedt, Chris Harvey, Roberta Harvey, Amina Kinkhabwala, Laura Lynch, Jaione Maiz, Paul Matthews, David Markowitz, Andrew Miri, Chris Moore, Peter Norgaard, Ilker Ozden, Meera Pratap, Greg Schwartz, Sara Sczepanski, David Shrom, Richard Sun, Fred Soo, Anuj Shah, Marylka Uusisaari, Linda Wilbrecht, Joyce Wondolowski. Thanks, guys, I wouldn't be in this field without you, and I wouldn't want to be here if you weren't! I especially want to thank Eugene Civillico for helpful collaboration during his time in the Wang lab, and consistent scientific and career advice during the years after.

TABLE OF CONTENTS

Abstract…….iii

Acknowledgements…….……...v

Introduction……1

Methods……...…..21

Results…….…….....28

Conclusions……...…….....54

Bibliography……..…….…...59

Introduction

History of cerebellar research

In terms of sheer number of cells the cerebellum makes up half of the brain, yet in a review as recent as 2009 concerning the history of cerebellar research, one of the major unsolved questions posed was “Finally, what does the cerebellum do?” (Glickstein, Strata, & Voogd, 2009). That this question is still unanswered is a testament to the multitude of behaviors to which the cerebellum contributes. This section describes landmark studies that show the importance of the cerebellum in movement, which has been well established, as well as behaviors that go well beyond movement. The goal of this section is to establish likely roles for the cerebellum in movement and cognition.

The cerebellum consists of the cerebellar cortex which projects to the deep cerebellar nuclei (DCN), in turn innervating extracerebellar structures. The cerebellum’s importance in movement has been known since the earliest studies of cerebellar function in 1824, when Flourens removed “successive layers” of cerebellar tissue from a pigeon. The pigeon’s ability to move became increasingly disordered until “…it was in a continual state of restlessness and agitation, but could never make any determinate movements (Ferrier, David, 1886; Thomson, 1884).

It took until 1917 for the first convincing evidence of cerebellar function in humans, when Gordon Holmes demonstrated that war-time gunshot wounds to the cerebellum produce movement deficits (Holmes, 1917). In this paper and subsequent studies, Holmes provides the first description of *all* of the major motor symptoms of cerebellar damage recognized today (Holmes, 1939). These range from the decreased muscle tone (hypotonia), the inability to

coordinate voluntary movements (ataxia), tremor, improper timing of movements (dysmetria), difficulty with alternating sequences of movement (dysdiadochokinesis), and vestibular symptoms such as the inability to maintain fixed gaze (nystagmus). Ballistic movements toward a target often over or undershoot. Motor production of speech is also affected: subjects have difficulty articulating words (dysarthria), often compounded by difficulty swallowing and changes in the rate, volume and timing of speech (Murdoch, 2010). Building on these studies, subsequent work has gathered substantial evidence confirming the cerebellum is involved in adjusting movement. Early microstimulation studies of the DCN suggested that the cerebellum could directly elicit movements (Schultz, Montgomery, & Marini, 1979). However, fibers of passage activated by the electrical stimulation may explain these results, as subsequent stimulation studies found only facilitation of movement (Delgado-García & Gruart, 2005; Soteropoulos & Baker, 2008). This remains a controversial question among experts in the field.

In addition to traumatic injury of the cerebellum, many of the same symptoms are present in genetic disorders of the cerebellum. There at least 43 known variants of Spino-Cerebellar Ataxia (SCA) stemming from a variety of gene mutations (Klockgether & Paulson, 2011; Matilla-Dueñas, 2012). Some of these are purely cerebellar; others involve damage to the cerebellum and other movement-associated structures such as the striatum. Symptoms can be equally debilitating as those produced by acute cerebellar damage. Recent findings have also implicated the cerebellum in at least one form of dystonia, symptoms of which include twitching, repetitive movement, and abnormal postures (Calderon, Fremont, Kraenzlin, & Khodakhah, 2011; LeDoux, Hurst, & Lorden, 1998; Neychev, Fan, Mitev, Hess, & Jinnah, 2008; Sadnicka, Hoffland, Bhatia, van de Warrenburg, & Edwards, 2012).

Though Holmes is rightly credited as the fountainhead of cerebellar research, his studies did not emphasize the crucial importance of the DCN within the cerebellar circuit. He concluded, on the basis of its small volume in comparison to the overlying cerebellar cortex, that "…in man and the primates the palaeocerebellum [DCN] is a relatively insignificant part of the whole" (Holmes, 1939). Contemporaneous work suggested otherwise. In a case study from 1940 the patient, a manual laborer by trade, was afflicted with cerebellar hypoplasia; a condition where the cerebellum does not mature normally after birth (Boyd, 2010). Little evidence can be found in the remarkably preserved medical records to suggest he suffered significant motor deficits. However, the description of his brain post-mortem describes the cerebellum as "…represented solely by a small nodule of nervous tissue, presumed to be paleocerebellar….." In short, this patient still had intact DCN. In evolutionarily older species the cerebellum consisted only of a "reflex arc" between sensory input regions, the DCN and structures efferent, without the overlying cerebellar cortex (Nieuwenhuys, Donkelaar, Nicholson, & Meek, 1998). The DCN are literally and figuratively at the core of cerebellar function.

The early studies of Holmes also did not describe a sensory role of the cerebellum. In part this oversight could be caused by the fact that these studies do not test the ability to use sensory information to learn new movement sequences or adapt existing motor programs to variations in external stimuli. It is now known that the cerebellum is involved in adaptive behavior, the process of transforming unexpected sensory events into expected events that can be anticipated. This involves generating an expectation about what is likely to occur and adjusting movements accordingly (Medina, 2011; Thach, Goodkin, & Keating, 1992). An example of how the cerebellum does this, and the crucial involvement of deep nuclei, is the well-studied example of eyeblink conditioning.

In this paradigm a light or tone stimulus (conditioned stimulus or CS) is paired with an airpuff or shock to one eye (unconditioned stimulus or US). With repeated pairing the animal learns to associate the CS with the impending US and blink the eye in time to block the puff of air (conditioned response, or CR). Information about the tone CS is conveyed from the auditory nucleus of the thalamus through the Pons which projects mossy fibers (MFs) to both the cerebellar cortex and DCN (see intro Figure.1, A). In the cerebellar cortex MFs terminate on granule cells which then synapse onto Purkinje cells (PCs) and molecular layer interneurons through parallel fibers (Figure.1, C) The US is conveyed from the trigeminal nucleus to PCs of the cerebellar cortex through the climbing fibers (CFs) of the inferior olive, which also send collaterals to the DCN. PCs inhibit neurons in the DCN. During acquisition of the CR, firing of neurons in a region of the DCN known as the anterior portion of the nucleus interpositus (AIP) increases, and this predicts how well the CR is learned (Berthier & Moore, 1990; Choi & Moore, 2003; Freeman & Nicholson, 1999; Nicholson & Freeman, 2002; Yang & Weisz, 1992). The cerebellar cortex is thought to be a major site of learning during eyeblink conditioning, as lesioning this region impairs the ability to learn the CS and produce appropriately timed CRs (Kalmbach et al., 2010; Ohyama & Mauk, 2001). The DCN are particularly critical for maintaining the learned response: If the cerebellar cortex is lesioned after learning has taken place the animal can still make a conditioned response (McCormick & Thompson, 1984), whereas lesioning the deep nuclei prevents consolidation of a learned motor response (McCormick, Clark, Lavond, & Thompson, 1982). Reversibly inactivating the DCN during training also prevents acquisition of the CR (Krupa, Thompson, & Thompson, 1993). This suggests that the DCN are a key site of plasticity, particularly at MF synapses conveying the tone information to DCN neurons.

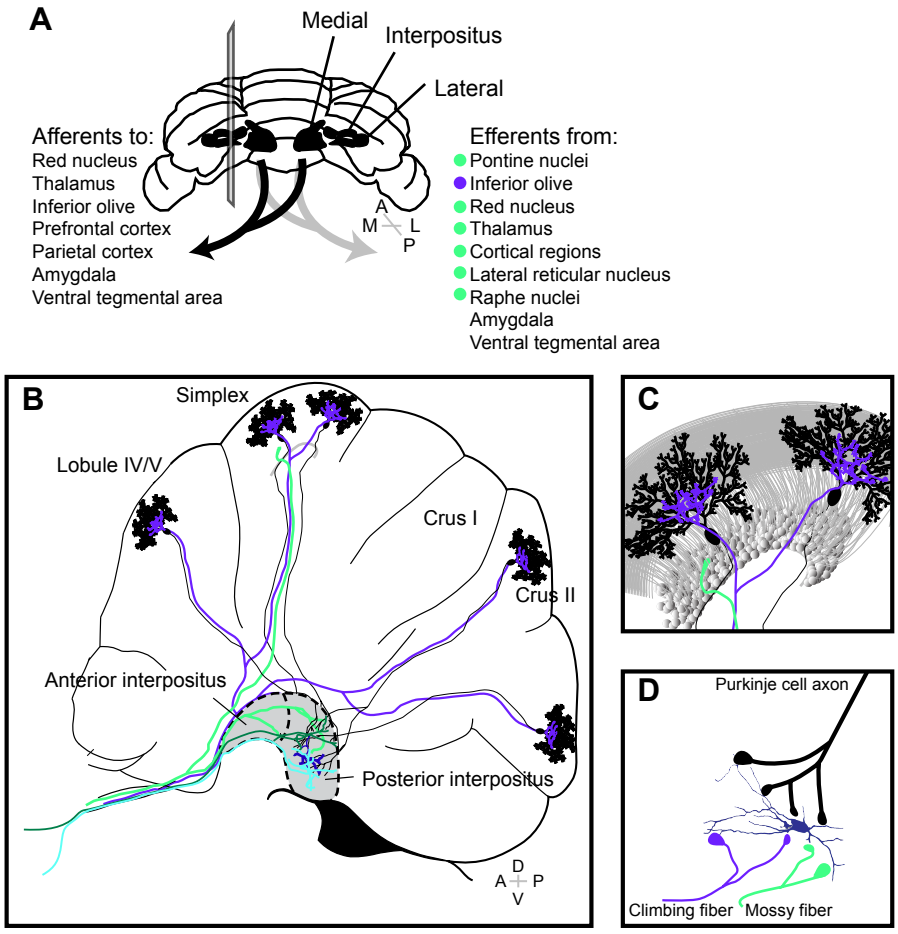


Figure 1. Cerebellar anatomy. A. Posterior view of the rat cerebellum showing DCN in silhouette. DCN project to the regions on left. Cerebellar cortex and DCN receive inputs from the regions on right via mossy fibers (MF) (●) or climbing fibers (CF) (●). B. Sagittal section through the nucleus interpositus, as indicated in A. Sagittal bands of PCs innervated by the same olivary axon (CF) across multiple lobules converge onto the same region of the DCN. C. Detail view of cerebellar cortex. Each PC is innervated by a single CF, forming ~500 active synaptic contacts. Up to four MFs innervate each granule cells, shown in gray. Granule cell axons extend into cortex and branch to form parallel fibers (PF) (—), which extend through the molecular layer ~0.9 mm in the coronal plane. Each PF crosses hundreds of PC dendrites, forming 6-8 synapses on each. D. Schematic view of location of PC, MF, and CF synapses onto DCN neurons. Neuron depicted represents all three classes of DCN neurons: excitatory or inhibitory projection neurons and local inhibitory interneurons. The majority of PC synapses arrive on the distal and proximal dendrites. Likewise, the majority of excitatory synapses are also on dendritic locations, so the ratio of excitatory: inhibitory inputs to the soma favors inhibition (Buisseret-Delmas & Angaut, 1988; Buisseret-Delmas, Angaut, Compoint, Diagne, & Buisseret, 1998; Chan-Palay, 1973a; Chan-Palay, 1973b; Chan-Palay, 1973c; Chan-Palay, 1977; Compoint, Buisseret-Delmas, Diagne, Buissseret, & Angaut, 1997; Groenewegen, Voogd, & Freedman, 1979; Middleton & Strick, 2001; Palay & Chan-Palay, 1974; Ruigrok & Voogd, 2000; Shinoda, Sugihara, Wu, & Sugiuchi, 2000; Silver, Momiyama, & Cull-Candy, 1998; Strick, Dum, & Fiez, 2009; Sugihara, Wu, & Shinoda, 1999; Sugihara, Wu, & Shinoda, 2001; Teune, van der Burg, de Zeeuw, Voogd, & Ruigrok, 1998; Wu, Sugihara, & Shinoda, 1999; De Zeeuw & Berrebi, 1995; de Zeeuw & Berrebi, 1996; De Zeeuw, Van Alphen, Hawkins, & Ruigrok, 1997).

Eyeblink conditioning is just one example of how learning in the DCN is involved in adaptive behavior. The cerebellum processes many types of expectation to adapt to changing stimuli including adjusting the timing and amplitude of movements (Medina, 2011) and altering reflex gain (Strick, Dum, & Fiez, 2009).

The examples discussed so far have focused on motor roles of the cerebellum. However, there is mounting evidence of cerebellar involvement in non-motor function. It is known that in primates the DCN project to many non-motor areas such as parietal and prefrontal cortices, the amygdala and VTA (Middleton & Strick, 2001; Phillipson, 1979; Watabe-Uchida, Zhu, Ogawa, Vamanrao, & Uchida, 2012). As with motor deficits, many of the non-motor symptoms are essentially problems of adaptive learning in different modalities. The greatest deficits are in the general category of "rule-based generation tasks" where constant modifications of expectations are required (Fiez, Petersen, Cheney, & Raichle, 1992; Stoodley, Valera, & Schmahmann, 2012). For instance, children who had benign tumors removed from the vermis of the cerebellar cortex and lateral cerebellar nucleus could learn sequences in a non-motor serial reaction time task, but could not flexibly respond when a new sequence was introduced (Berger et al., 2005). Verbal association tasks, a similar paradigm in the language domain, are also a challenge for cerebellar patients (Stoodley et al., 2012). Adults with cerebellar damage show many cognitive-linguistic symptoms such as agrammatic speech, decreased verbal fluency, and the inability to learn new associations between words (Drepper, Timmann, Kolb, & Diener, 1999; Fiez et al., 1992; Murdoch, 2010). MRI evidence suggests that parts of the cerebellum are activated during complex visuo-spatial tasks (Stoodley & Schmahmann, 2009; Stoodley et al., 2012) and there is evidence of impairment on these tasks in cerebellar patients (Levisohn, Cronin-Golomb, & Schmahmann, 2000). Children with vermal damage also show affective symptoms such as labile

and irritable moods and feeling “easily overwhelmed” by the tasks (Levisohn et al., 2000; Schmahmann, 2004; Stoodley et al., 2012). The lateral hemispheres of the cerebellar cortex, which project to the lateral nucleus, have been linked to higher cognition (Desmond, Gabrieli, & Glover, 1998; Joyal et al., 2004; Schmahmann, 1998). Consistent with these studies, in children with chromosomal abnormalities affecting the cerebellum, decreased volume of the right lateral hemisphere was associated with deficits of expressive language and lower scores on a general cognitive test (Bolduc et al., 2012).

Some hypothesize that social development depends on accurately perceiving the precise timing of the movements of others, and the inability to perceive these subtleties may be one of the aberrant features in individuals on the autism spectrum (Klin, Lin, Gorrindo, Ramsay, & Jones, 2009). A cerebellar basis contribution has been suggested based on the cerebellum’s involvement in adaptive learning and the observation that congenital cerebellar abnormalities, particularly those associated with decreased vermal volume, have been linked to autism (Bolduc et al., 2012; Courchesne et al., 1994; Gerlai et al., 1996; Klin et al., 2009; Pierce & Courchesne, 2001). In addition, cerebellum-specific deletions of a gene linked to an autism-like disorder in humans causes autisto-mimetic behavioral phenotype in mice (Tsai et al., 2012).

Because so many cerebellar disorders involve learning we must ask the question: How does learning occur in cells of the deep nuclei? How do active dendrites contribute to this learning?

Active dendrites: Examples and implications for synaptic plasticity

In the classical view, active propagation was the province of the axon. In this view, dendrites convey input to the soma by passive voltage spread, where the combined voltage

change can bring a spike initiation zone called the axon hillock to threshold for firing (Jack, Noble, & Tsien, 1983). The axon hillock is rich in voltage-gated sodium channels, so that a small change in voltage is amplified via positive feedback. Then the action potential arises abruptly, and is propagated down the axon to the next neuron.

While this is true for axons, it does not take into account that dendrites are now appreciated to express not just neurotransmitter receptors, but also many voltage-gated channels. Therefore they are also capable of generating voltage dynamics.

The classical example of dendritic electrogenesis is the cerebellar Purkinje cell (PC). Llinas and Sugimori made sharp electrode recordings from various distances from the soma of PC dendrites. If they strongly depolarized the dendrites through the recording electrode or synaptically stimulated the climbing fiber pathway, which provides a large all-or-none input (intro Figure.1C), they could cause the dendrites can fire action potentials (Llinás & Sugimori, 1980). These dendritic APs were generated when depolarization caused the opening of numerous voltage-gated dendritic calcium channels, which allowed extracellular calcium to enter the cell, causing a burst of dendritic calcium spikes. Subsequent research has shown that calcium spikes arising from the CF stimulus are not just attenuated versions of somatic spikes. Davie and colleagues found that the number of dendritic spikes measured on a recording electrode placed on the Purkinje cell dendrite differed from the number of spikes measured on a somatic electrode, during the same CF stimulation (Davie, Clark, & Häusser, 2008). These dendritic spikes are decoupled from the somatic spikes.

PCs are not the only cells with excitable dendrites, nor are calcium spikes the only form of dendritic excitability. Another extensively studied form of dendritic activity is boosting of the

backpropagating action potential (BAP), which can occur through calcium or sodium channel dependent mechanisms.

Stuart and Sakmann observed that sodium spikes could back-propagate further into the dendrites than passive models suggested (Stuart & Sakmann, 1994). The mechanism for this amplification in cortical and hippocampal pyramidal cells was through dendritic sodium channels that open when depolarized by the BAP allowing it to spread up to several hundred microns into the dendrites. BAPs in dopamine neurons of the substantia nigra show even less attenuation; these neurons have particularly wide APs and few dendritic branch points both of which enable backpropagation (Häusser, Stuart, Racca, & Sakmann, 1995). At the other extreme are cerebellar PCs where the BAP is degraded by 50% only 50 μm from the soma (Stuart & Häusser, 1994). PC dendrites express no voltage-gated sodium channels. However, in this case the BAP is not necessary for amplifying dendritic voltage because, as described above, PCs fire dendritic calcium spikes.

One of the main reasons active dendrites are interesting is their ability to contribute to synaptic plasticity, the cellular basis of learning. In areas crucially involved in learning, such as the deep cerebellar nuclei, this is particularly important. Synaptic plasticity can be broadly defined as modifications in the strength of synaptic connections between neurons. Learning rules at synapses, such as Hebbian and spike-timing dependent plasticity, are driven by voltage. Neurons use ion channels expressed on their dendrites to change the voltage where synapses are located, dictating the conditions under which plasticity can occur. Further, active dendrites can generate nonlinearities in the dendritic voltage response to inputs, enabling inputs at some locations to be amplified while attenuating others (Mel, 1993). For example, voltage-gated conductances in pyramidal cells allow greater summation of inputs arriving on one dendritic

branch than synapses on separate branches (Polsky, Mel, & Schiller, 2004). The unit of learning is not the single neuron, but rather the dendritic compartment. In short, dendritic calcium spikes can also amplify distal inputs so they are larger than those proximal, extremely counterintuitive in a passive dendrite (Magee & Cook, 2000). Dendritic excitability opens many possibilities for synaptic integration.

The voltage dynamics necessary to change synaptic strength depend on the properties of signaling molecules necessary for plasticity in different cell types. For example, spike-timing dependent plasticity (STDP) (Abbott & Nelson, 2000) at CA3-CA1 synapses of the hippocampus depends almost entirely voltage-dependence of NMDA receptors (Magee & Johnston, 1997). Briefly, the rule of this type of plasticity at this synapse is that if two cells are connected and the postsynaptic cell fires shortly after the presynaptic cell, synaptic connections between these cells will be potentiated. This potentiation is also known as Hebbian plasticity. If this order is reversed but the events are still closely spaced in time the synapses are depressed, whereas if the stimuli are separated in time the synaptic weight does not change. This is because NMDA receptors require the coincidence of depolarization (in this case the postsynaptic spike) and glutamate binding to open. Both of these conditions must be satisfied simultaneously to allow enough calcium to enter the cell and initiate the complex chain of events that ends in increased synaptic strength.

The canonical model of STDP at this synapse doesn't take into account that neurons have dendrites. Consider the case of a synapse at a very distal dendritic location. If somatic spikes do not back-propagate into the dendrites to depolarize this synapse there would be either no potentiation, or synaptic depression (Sjöström, Rancz, Roth, & Häusser, 2008). For potentiation to occur at this distal synapse, some means of changing the voltage in the dendrite is needed,

either boosting of the BAP or, as in PCs, calcium spikes in the dendrites. Dendritic excitability is a critical link between theoretical ideas about Hebbian plasticity and implementing them in actual neurons (Mel, 2002).

An analogous situation exists in DCN neurons: The majority of excitatory MF and inhibitory PC synapses are located on the dendrites, at varying distances from the soma. It is not known how dendritic voltage could be regulated in these neurons. For instance, there is no *a priori* reason to assume the BAP would propagate well in DCN dendrites. On one hand there is no evidence that DCN neurons express dendritic sodium channels, rather, they express many dendritic potassium channels, which could shunt the BAP (Anderson et al., 2010; Raman, Gustafson, & Padgett, 2000). Further, morphologically they possess fewer branch points than cerebellar PCs and passive models suggest the electrotonic distance of dendrites is long, all factors which could enhance BAPs. (Steuber, De Schutter, & Jaeger, 2004) However, DCN APs are often extremely narrow because of fast potassium channel expression, and AP width is a major determinant of BAP efficiency (Golding, Kath, & Spruston, 2001). In contrast, there is far more evidence that DCN neurons could produce dendritic calcium spikes, and that these might be necessary for at least one form of plasticity in this brain region.

Learning in the DCN

There are several types of plasticity have been demonstrated thus far in DCN neurons, all of which depend on voltage. Consistent with observations that DCN neurons increase their firing during the acquisition of condition eye-blink responses (Freeman & Nicholson, 1999; Nicholson & Freeman, 2002; Yang & Weisz, 1992), changes in intrinsic excitability and strengthening of MF synapses onto DCN neurons have been demonstrated (Aizenman, Manis, & Linden, 1998;

Pugh & Raman, 2006; Zhang, Shin, & Linden, 2004). PC inhibition from the cerebellar cortex is the only direct means by which the cerebellar cortex can instruct the nuclei. PC synapses also have been shown to undergo use-dependent synaptic plasticity (Aizenman et al., 1998).

Excitatory synapses (most likely a mixed population of mossy fiber and climbing fiber collaterals) can be strengthened using a protocol designed to mimic the timing of MF and PC inputs during eyeblink conditioning. This paradigm involves repeated pairing of trains of synaptic stimulation with brief somatic hyperpolarization or synaptic inhibition (250 ms) to induce LTP. Stimulating excitatory and inhibitory afferents with the same temporal pattern also induces LTP (Zheng & Raman, 2010).

The timing rule for this LTP induction does not match those shown to induce LTP in the hippocampus in that synaptic stimulation coincident with post-synaptic depolarization or NMDA-receptor activation does not potentiate DCN neurons (Aizenman & Linden, 1999; Pugh & Raman, 2006; Pugh & Raman, 2009). Instead, two conditions must be met; synaptic activity coincident with inhibition, followed by disinhibition. Some of the molecular effectors for this type of plasticity are known. In order for LTP to occur intracellular calcium is necessary to activate the enzymes αCAMKII and calcineurin (Person & Raman, 2010). Calcium influx through NMDA receptors is necessary but not sufficient for plasticity at this synapse (Person & Raman, 2010). Further, it is unlikely that the NMDA receptor is acting like a coincidence-detector, because DCN neurons express a form of the NMDA receptor that can open at negative voltages (Anchisi, Scelfo, & Tempia, 2001). The missing piece in explaining MF LTP in the DCN is a robust source of calcium sufficient to activate αCAMKII, suggesting some other mechanism must exist for amplifying voltage and allowing calcium entry near the synapse.

Both MF and PC synapses can undergo plasticity that is activity-dependent and calcium dependent, but does not rely coincident input from the other respective pathway (Aizenman et al., 1998). When PC afferents are repeatedly stimulated this evokes a burst of spikes following the rebound from inhibition. The rebound is caused by low-voltage activated (LVA) calcium channels, which will be discussed at length in the next section (Aizenman & Linden, 1999; Llinás & Mühlethaler, 1988; Molineux et al., 2008). Stimulating PC synapses at high frequencies to evoke repeated rebound spiking (termed "burst protocols") increases the size of PC inhibitory post-synaptic potentials (IPSPs). Likewise, stimulating excitatory synapses, which also evoke rebound bursting, has the same effect on PC synapses. The common theme among these protocols is that cells are first hyperpolarized to prevent spiking, then brought to spike threshold by either direct excitation, or by rebound from inhibition. Conditions that do not permit rebound spiking, either by injecting hyperpolarizing current to prevent cells from firing or by blocking sodium channels cause LTD (Aizenman, Huang, Manis, & Linden, 2000; Aizenman et al., 1998). This suggests a larger change in voltage is required for LTP than LTD. LTP burst protocols also drive calcium influx in the soma and proximal dendrites. Chelating intracellular calcium blocks both LTP and LTD (Aizenman et al., 2000).

The same excitatory and inhibitory burst protocols that induce plasticity at PC synapses paradoxically also cause increases in the excitability of DCN neurons. After LTP burst protocols neurons fired more spikes when injected with depolarizing current, a phenomenon termed long-term potentiation of intrinsic excitability (LTP-IE). This stimulation also causes calcium to accumulate in the dendrites during the burst stimuli (Zhang et al., 2004).

All these forms of plasticity are voltage dependent. Excitatory synapses are located at greater density on the dendrites than the soma (Chan-Palay, 1973b). PC afferents outnumber

excitatory inputs on the soma, but the majority of PC synapses are also on distal dendrites (De Zeeuw & Berrebi, 1995). Previous work has used somatic recordings and calcium imaging at proximal sites, so factors that enable voltage change at the location of the majority of synapses are still not understood. Since it is possible for DCN neurons to undergo plasticity a mechanism must be present for amplifying voltage in the dendrites. In other neurons this has been accomplished by a variety of means, including boosting backpropagating APs using voltage-gated sodium and calcium channels, or amplifying distal inputs with regenerative calcium spikes.

Evidence for active dendrites in the DCN.

There is prior evidence of dendritic calcium entry in deep nuclear neurons. Given that inhibitory PC synapses are the most numerous inputs to DCN dendrites it should be a mechanism that can be triggered at least in part by inhibition. One candidate is low-voltage activated T-type calcium channels. These channels are activated at moderate voltages but require hyperpolarization to first remove inactivation so the channels can open (Perez-Reyes, 2003). Studies of cultured DCN neurons did not observe T-type calcium current, though it is present in cells recorded from acute slices (Raman et al., 2000). This could be explained if T-type channels are preferentially located on the dendrites, which are underdeveloped in culture (Gauck, Thomann, Jaeger, & Borst, 2001). Immunostaining for Cav3.3 and 3.1 T-type channel isoforms finds that these markers are expressed in the soma of DCN neurons, and that:

> Ca_v3 immunolabel in the DCN neurons… exhibited a diffuse interstitial label within the boundaries of the nuclei; a label that was entirely absent when Ca_v3 antibodies were omitted or preadsorbed with purified protein…. The source of the diffuse label was not strictly identified, but likely reflects the extremely dense network of small-diameter axonal, dendritic, and glial processes in the DCN (Molineux et al., 2006).

This suggests that T-type channels are located on dendritic regions of DCN neurons, as well as the soma. Some DCN neurons fire a burst of spikes following somatic hyperpolarization or inhibitory synaptic stimulation (Aizenman & Linden, 1999; Czubayko, Sultan, Thier, & Schwarz, 2001; Jahnsen, 1986). This response to hyperpolarization has been shown to be well correlated with T-type calcium channel expression, with neurons that fire high-frequency bursts following hyperpolarization termed "transient bursters" (TBs) expressing the Cav3.1 T-type channel isoform and those that do not burst termed "weak bursters" (WBs) expressing Cav3.3 (Molineux et al., 2006; Molineux et al., 2008). Current through T-type calcium channels (I_T) has been directly measured using a waveform that simulates repeated PC stimulation (Engbers et al., 2011). Hyperpolarizations between 100-300 ms generated 5-15% of the maximum available I_T in both WBs and TBs, (although the total I_T is smaller in WBs). In current clamp, hyperpolarizing steps to -72 mV also generated a rebound bursts of ~100 Hz in TBs, as seen in other previous reports *in vitro* (Aizenman & Linden, 1999) and in awake, behaving mice *in vivo* (Hoebeek, Witter, Ruigrok, & De Zeeuw, 2010). This evidence suggests that T-type channels are expressed in DCN neurons and can be activated in physiologically relevant situations.

There are several lines of evidence that support the idea of LVA channel being the source of post-inhibitory calcium influx in the dendrites. Gauck Thomann & Jaeger observed that LVA barium currents are greater in the dendrites than in the soma. Voltage-clamp protocols designed to preferentially activate LVA or high-voltage activated (HVA) current suggest that there is a larger change in barium indicator fluorescence (%ΔF/F) in proximal and intermediate dendrites relative to the soma, whereas the converse holds true for HVA current (Gauck et al., 2001). This finding could be distorted by poor space clamp, the technical difficulty of control voltage at sites distant from the recording electrode such as dendrites; however, in passive models of DCN

neurons the dendritic voltage deviation is ≤ 1 mV for voltages used in this study. Further, calcium imaging in proximal dendrites in current clamp where assumptions of good space clamp are not necessary also support this view. In somewhat proximal dendrites of primarily weak bursters calcium transients following removal of hyperpolarization barely overshoot the steady-state calcium levels present during tonic firing (Zheng & Raman, 2009). This additional calcium entry would not differ significantly from increased calcium caused by the NMDA receptor activation during excitatory synaptic stimulation and thus would be insufficient to activate αCAMKII.

A final piece of evidence suggesting that there could be calcium spikes in the dendrite, possibly driven by LVA channels, is the observation that when neurons are held at a hyperpolarized potential (sufficient to remove inactivation from T-type channels) then driven to fire "bursts" of spikes repeatedly by either EPSP or IPSP stimulation, calcium accumulates in the dendrites more than in the soma (Zhang et al., 2004). While providing useful information about the spatial pattern of calcium entry, the imaging is on a timescale that does not give much information about the amount or kinetics of calcium entry during a single rebound burst. Interestingly, this pattern of synaptic stimulation also increases the intrinsic excitability of neurons, such that they fire more spikes in response to a test pulse following the "burst" stimulation.

There is also an argument to be made supporting the necessity of dendritic calcium signals based on the timing of plasticity. The timing rule at deep nuclear synapses is similar in precision to that for Purkinje cell LTD, though inverse. As previously discussed, NMDA receptors in the DCN could not create such a precise timing rule. Further, calcium influx through LVA channels is subject to many of the same temporal smearing problems as synaptic

stimulation. For instance, if neurons relied on rapid spiking to drive calcium entry through L-type channels calcium would slowly increase or decrease up to new levels, following the spike rate. In contrast, LVA channels open rapidly then inactivate, so stimuli that activate them could provide a brief, large spike of calcium in the dendrites. This event would occur rapidly and only under the right conditions of synaptic input. There is precedent for this type of rapid, T-type driven dendritic calcium spike in several other neuronal types.

T-type Ca^{2+} channels in other neuronal types: relevance for DCN.

T-type calcium channels are present in many types of neurons throughout the brain (McKay et al., 2006). I_T-driven dendritic calcium transients that are relevant to the function of neurons in vivo occur in several neuronal types such as thalamic reticular neurons (TRN), and olfactory mitral cells (Crandall, Govindaiah, & Cox, 2010; Johnston & Delaney, 2010). The role of dendritic calcium spikes in these types of neurons may provide insights for what one might expect in the deep cerebellar nuclei, where less is known about their behavioral function and the precise organization of inputs. In these cell types, activating T-channels has been shown to produce large dendritic calcium spikes. The location and properties of these channels have some interesting implications for dendritic integration and plasticity.

A common feature of TRN neurons and mitral cells is that they have long dendrites, several hundred microns in the TRN and >500 μm for mitral cell primary dendrites. Without some mechanism to amplify distal inputs they would have little effect on the firing properties of these neurons, as distal EPSPs would be significantly attenuated by the time they reach the soma. Additionally, both these types of neurons have been shown to burst *in vivo* (Contreras, Curró Dossi, & Steriade, 1993; Sobel & Tank, 1993).

TRNs fire somatic bursts that are accompanied by large dendritic calcium transients when the soma is depolarized from -80 mV by current injection. These transients are not attenuated by blockers of sodium channels or L-type calcium channels (TTX or nifedipine), but are almost completely abolished by the T-type antagonist mibefradil, suggesting they are T-type in origin. Rapid application of glutamate results in calcium transients of similar amplitude to those evoked with somatic current injection, and the amplitude of these transients remains constant in the presence of TTX, but was greatly attenuated by mibefradil. Calcium transients in distal dendrites are ~143 % larger than in proximal dendrites. Interestingly, though the distal dendrites are smaller than the proximal dendrites, dendritic diameter correlates only weakly with the size of the calcium transients. This suggests that the large calcium transients observed at distal locations are a product of increased I_T at those locations, rather than an artifact because of a greater surface-to-volume ratio in distal dendrites.

More is known regarding the organization of afferents in the thalamic reticular nucleus compared to the DCN. Fibers from cortico-thalamic and thalamo-cortical projection neurons are spatially segregated by modality. Crandall et al., put forth the hypothesis that because of this organization, and the fact that cortico-thalamic projections preferentially synapse on distal dendrites of TRN neurons, that EPSPs would be the most increased by the presence of T channels, thus privileging distal inputs, allowing robust “top-down” control. Fibers from one modality that synapse onto distal dendrites might thus influence sensory processing of another modality. This is borne out in the observations from several reports that TRN neurons can respond to more than one sensory modality *in vivo* (Sugitani, 1979; Yu, Xu, He, & He, 2009) and are under attentional control (McAlonan, Cavanaugh, & Wurtz, 2006; McAlonan,

Cavanaugh, & Wurtz, 2008). New evidence has been published that also supports multi-modal integration in the TRN (Yu, Meng, Xu, & He, 2011).

As in the TRN, DCN dendrites extend 200 μm or more in many directions, sometimes crossing borders between nuclear subregions, such as the interpositus anterior and posterior, or dendrites originating in the dentate *pars compacta* that invade other regions of the dentate (Chan-Palay, 1977). Because little is known about the different subdivisions of the individual deep nuclei beyond simple anatomical distinctions, it is less clear whether PC inputs to distal and proximal dendrites convey different information. In vivo studies showing differences in the activity of very small cerebellar microzones suggest this may be the case, but further study is needed (Ozden, Sullivan, Lee, & Wang, 2009).

In olfactory mitral cells calcium transients in distal dendrites can be initiated by the back-propagating action potential, which has been shown to propagate unaltered to the distal dendrites (Bischofberger & Jonas, 1997) or by glutamatergic synaptic activation. In vivo, the membrane potential of these neurons oscillates with respiration such that the voltage is periodically in a range where T-type channels are capable of being activated and are not inactivated, termed a "window current". During olfactory stimulation a long-lasting depolarization (LLD) is evoked in mitral cells, accompanied by a rise in calcium in the distal dendrites. The calcium influx generated by the LLD is primarily mediated by mGluR activation of I_T and NDMA receptors. Factors that regulate calcium influx in distal dendrites may be important for converting the LLD into spiking. These neurons can also release neurotransmitter from their dendrites, which is also regulated by dendritic calcium influx. Similar to the amplification of glutamatergic EPSPs observed in olfactory mitral primary dendrites, T-type calcium channels have been found to

amplify PC IPSCs in DCN neurons and cause DCN neurons to burst (Engbers et al., 2011). However, it is not yet known whether they can drive dendritic spiking in DCN neurons.

The existing evidence for the possibility of dendritic calcium transients, as well as the requirement for such a signal in known forms of DCN plasticity lead us to perform experiments to test whether these signals exist, and how they compare to calcium influx generated through HVA channels activated by the BAP.

Methods

Rationale for using young animals

P13-19 day old Sprague-Dawley rats (Charles River Laboratories, Wilmington MA) were used in all studies contained in this dissertation. There are several reasons for using juvenile animals. First, this work exclusively examines intrinsic conductances, which have been suggested to be similar to adult animals at this stage (Gardette, Debono, Dupont, & Crepel, 1985). Further, recordings from deep nuclear neurons in P13-16 brain slices show electrophysiological behavior consistent with recordings from mature guinea pig neurons in a semi-intact preparation (Aizenman & Linden, 1999; Llinás & Mühlethaler, 1988). Recent results from animals up to one month of age in brain slices at physiological temperature further indicate a lack of obvious difference in evoked Purkinje cell and mossy fiber PSPs or the ability to undergo LTP between young and old animals (Person & Raman, 2012). Second, comparison with prior work required animals of a similar age range (Aizenman, Huang, & Linden, 2003; Czubayko et al., 2001; Molineux et al., 2008; Uusisaari, Obata, & Knöpfel, 2007; Zheng & Raman, 2009). The deep nuclei are heavily striated with myelinated fibers of passage, making it difficult to visualize cells for recording. This age range is preferred because the dense extracellular matrix that forms in older animals impairs visibility even further. Additionally, the deep nuclei have the highest expression of extracellular matrix proteoglycans of any brain region, consisting primarily of hyaluronan molecules, which form large complexes with chondroitin and tenascin-R molecules (Carulli et al., 2006; Toole, 2004). The hyaluronan remains covalently bound to the soma after it is extruded, making it difficult to form the gigaohm seal necessary for patch clamp recording.

Slicing procedure.

All procedures were approved by the Princeton University Institutional Animal Care and Use Committee. Animals were anesthetized with isoflurane and decapitated. The cerebellum and brainstem were removed and immersed in ice-cold ACSF containing (in mM): 126 NaCl, 3 KCl, 1 NaH_2PO_4, 25 $NaHCO_3$ 20 D-glucose, 2 $CaCl_2$, 1 $MgCl_2$ oxygenated with 95% O_2 / 5% CO_2. Several other solutions were tested including a K^+ gluconate solution, substituting the NaCl for choline chloride or sucrose, adding kynurenic acid to the slice incubation chamber and a Ca^{++}/Mg^{++}-free solution. None of these produced a noticeable improvement, and those recordings are not included in this dissertation.

The tissue block was transferred to a dissecting dish filled with ice-cold ACSF, the dura removed and the brainstem severed at the peduncles. The remaining cerebellum was bisected sagittally through the vermis with a #21 blade scalpel (FST, Foster City, CA). Both halves were blotted with filter paper and mounted using cyanoacrylate glue on a Leica VT1000S vibratome (Nussloch, Germany) set to speed 1-2.5 and frequency 8-9. 250-300 μm thick sagittal slices were cut using ceramic blades (Lafayette Instrument Company, Lafayette, IN). Slices were taken at distances of 1.8 to 4.5 mm medial from the most lateral extreme of the paramedian lobule. Slices were incubated for 45-60 min at 34˚C and then brought to room temperature.

In occasional cases P19 rats were sliced following the same procedure above except that dissection and slicing were performed at 34˚C as described in previous literature (Dingledine, Dodd, & Kelly, 1980; Person & Raman, 2012). Likewise, several recordings included here were made from coronal slices where the entire cerebellum was removed and the anterior face of the cerebellum was glued to the specimen holder.

Locating cells within the deep nuclei

In order to determine the location of recorded cells each slice was imaged after recording using an Olympus BX51WI epifluorescence microscope with a MicroFire camera (Olympus, Center Valley, PA). Briefly, the slice was transferred to a slide and wet-mounted in ACSF. Filled cells were then photographed under epifluorescence and 4-10 bright or darkfield images were obtained. These images were then tiled and the slice was aligned with the corresponding slice image in Figure 2. The location of the slice was also noted during the slicing procedure, beginning with 1.8 mm medial from the most lateral position of the paramedian lobule, ending at 4.5 mm medial from this position. These coordinates were aligned with coordinates in the Paxinos & Watson atlas 4th edition based on visual approximation, and converted to mm from the midline (Paxinos & Watson, 1998). Paxinos coordinates are reported in figures and text. Because these measurements were made in living tissue and the atlas is based on a fixed specimen of a different age, these coordinates should be considered approximate only. In particular, the border between the medial portion of the dentate nucleus and the interpositus nucleus cannot be determined accurately because there are no obvious histological landmarks exist in the parasagittal plain, so cells in this region were assigned to the lateral nucleus (Czubayko et al., 2001).

Electrophysiological recording and calcium imaging.

Slices were placed in an immersion recording chamber (Warner Instruments, Hamden CT) at room temperature or 33˚C and perfused with ACSF at a rate of 2-4 mL/min. Cells from all three cerebellar nuclei were whole-cell patch-clamped (borosilicate pipettes, 2-8 MΩ) using a pipette solution containing (mM) 133 methanesulfonic acid, 7.4 KCl, 0.3 $MgCl_2$, 3 Na_2ATP, 0.3 Na_3GTP, and 0.02 EGTA, pH 7.3 with KOH, 290 mOsm. For calcium imaging the EGTA was

replaced with 0.2 mM Calcium Green-1 or Fluo-5F (Invitrogen, Carlsbad, CA). In some cases 10-30 μM Alexa 594 or 568 (Invitrogen, Carlsbad, CA**)** was added.

Cells were accepted for recording if they fired tonically at zero current, generated overshooting spikes, had input resistance of 100-1700 MΩ (446.4 ± 342.1, mean ± S.D.) and access resistance of 2-10 times pipette resistance, and had visible dendrites after 45 min of whole-cell recording. Two cells located in the lateral nucleus that did not spike at zero current were accepted because their other whole-cell parameters were otherwise within acceptable limits and a subpopulation of glycinergic interneurons with this behavior has been reported to exist in the literature (Uusisaari & Knöpfel, 2010). Several cells with input resistance of ~80 MΩ were also accepted, as otherwise their behavior was indistinguishable from other cells in the dataset.

Imaging was done on a custom two-photon microscope running CfNT (R. Stepnoski, Bell Labs, Murray Hill, NJ, USA; M. Müller, Max Planck Institute for Medical Research, Heidelberg, Germany) or Scanimage 3.6 software (Pologruto, Sabatini, & Svoboda, 2003) by frame (500 ms), band (16 ms), or line (2 ms) scanning. Cells were loaded with calcium indicator dye through the recording electrode for a minimum of 20 minutes and an average of 45 minutes before imaging to allow distal dendrites to fill. Briefly, in cases where imaging was done in movie mode, attempts were made to find a planar dendrite and image different locations simultaneously. In cases where band or line scans were used either the scan orientation was positioned such that multiple regions of the dendrite were included, or multiple regions were scanned separately at different points along a dendrite. This situation yielded better results as lower laser power could be used for proximal regions which was less damaging to the cell. For distal regions, often ~ 100 μm beneath the slice soma higher laser power could be used to resolve thin dendrites deeper in the tissue. Bandscans were used most frequently because they were more

resistant to small changes in position of the dendrites than linescans and the scan position was constantly refocused between scans to ensure the same position on the dendrites was imaged.

Electrophysiological signals were recorded using either an Axopatch 200B (2 kHz filtering) and digitized with National Instruments hardware controlled by Igor Pro 6 (Wavemetrics, Oswego NY) using custom routines and the NiDAQ Tools package. In some cases, signals were recorded using a Multiclamp 700A amplifier, digitized with a Digidata 1320 and acquired using PClamp software (Molecular Devices, Sunnyvale, CA). All recordings reported in this dissertation were made in current clamp mode, with the exception of voltage pulses used to measure series and input resistance. Transient bursting neurons were defined as firing at least 2 spikes at >10 times the baseline firing rate after removal of a hyperpolarizing current step to < -70 mV of 200-1000 ms duration (Molineux et al, 2006) The remaining neurons were classified as weak bursters. Some cells were also stimulated with hyperpolarization ending with ramps of varying slopes to assess whether the rate of removal of hyperpolarization affected the rate of the rebound burst. Occasionally, constant-charge depolarizing pulses of 10 pC were given to neurons that were tonically spiking, to determine if this stimulation could elicit firing comparable to a rebound burst.

Pharmacology experiments and chemicals.

NNC 55-0396 dihydrochloride (Tocris Bioscience, Ellisville, MO), tetrodotoxin, and kynurenate (Ascent Scientific, Princeton NJ) were applied to slices by gravity perfusion. Other chemicals were from Sigma-Aldrich unless otherwise noted.

For treatment with phorbol 12-myristate-13-acetate (PMA), slices were incubated in oxygenated ACSF containing 200-400nM PMA at 37˚C for 10 minutes then transferred to the

recording chamber. PMA was dissolved in dry DMSO at 1 mM, aliquoted and stored at -80˚C. Before use, aliquots were thawed and sonicated for 10 minutes then added to ACSF immediately before incubating slices in PMA solution. PMA binding of PKC is irreversible, so slices were used up to 8 hours after PMA treatment.

Data analysis.

Electrophysiology and imaging data were analyzed using Igor Pro and Matlab 2008a (The Mathworks, Natick, MA) using custom routines written by Eugene Civillico and Eve Schneider. In the case of CfNT, data functions written by Thomas Euler were incorporated into functions written by Eugene Civillico. Membrane voltage was corrected post-recording for liquid junction potentials calculated using JPCalc (Molecular Devices, Sunnyvale, CA). Slices were photographed for documentation of DCN and the location of recorded neurons.

To express indicator signals in comparable units, ΔF/F signals for fluo-5F were converted to equivalent changes in Calcium Green-1 fluorescence by a three-step procedure: (1) ΔF/F values were calculated as a function of free [Ca] for each indicator assuming $[Ca]_{rest}$, free=50 nM, KD=1.0 uM and Rf=220 for fluo-5F (Sarkisov & Wang, 2008) and KD=0.25 uM and $Rf=F_{max}/F_{min}=20$ for Calcium Green-1 (Haugland, 2002). Calcium Green-1 KD and Rf were adjusted to give the observed $(\Delta F/F)_{max}$, ~350%. (2) For each indicator, total molar calcium change leading to a given $[Ca]_{free}$ was calculated assuming an endogenous buffer with kappa=100 (Helmchen, Imoto, & Sakmann, 1996; Neher & Augustine, 1992) and 150 μM of indicator dye in the dendrites. (3) The ΔF/F value for fluo-5F was converted to an equivalent value for Calcium Green-1 corresponding to the same total molar calcium change. The net effect of this procedure was a near-linear downward scaling of ΔF/F by a factor of 3.0. This conversion

was used to express transients two weak bursters filled with calcium green-1 treated with TTX (figure 4, B) in units of fluo-5F.

Where significance testing was necessary, the following tests were used. Kolmogorov-Smirnov (K-S) tests were used to assess the probability that two distributions were the same when there was no reason to assume the normality of either distribution. P-values for K-S tests were calculated using the method of Marsaglia (Marsaglia G, Tsang WW, Wang J, 2003). In cases comparing measurements from the same cells in different conditions, such as pharmacology experiments, paired 2-tailed Student's t-tests were used assuming equal variance and a 2-tailed hypothesis. To compare whether the means of two distributions differed from each other when measurements were made from different cells, sometimes resulting in unequal sample sizes, unpaired Student's T-tests were used assuming unequal variance and a 2-tailed hypothesis. To correct for multiple comparisons criteria for significance was set by Bonferroni-correcting the familywise alpha for the number of comparisons. To test whether the correlation between two variables was significantly different from zero, linear correlations were used, and P-values were calculated using the assumption of a 2-tailed hypothesis. All data are reported in the text as mean ± S.D. and error bars in figures are displayed as SEM unless otherwise specified.

Results

Rebound response is heterogeneous in the DCN

The most striking electrophysiological characteristic of DCN neurons is their response to the removal of hyperpolarization: a subset of cells generate what are known as “rebound” bursts. Rebound bursts have been shown to correlate with the presence of voltage-gated T-type calcium channels, which can support dendritic calcium spikes. As a first test for this conductance, we quantified changes in neuronal firing rates in response to hyperpolarization.

Upon removal of hyperpolarization, DCN neurons either resume their pre-hyperpolarization baseline firing rate, fire at an elevated rate, or generate a “rebound burst,” comprising a brief burst of 2-6 spikes at frequencies ranging from 50-600 Hz and often followed by an after-hyperpolarization lasting 70-140 ms. Figure 1A shows example traces from the extremes of this continuum. Previously, cells that fire rebound bursts have been termed transient bursters (TBs), and other cells weak bursters (WBs) (Molineux et al., 2006). These firing patterns have been shown to correlate with the expression of Cav3.1 (TBs) and 3.3 (WBs) (Molineux et al., 2008). An alternate classification, based on firing rate alone, has also been also been used (Alviña, Walter, Kohn, Ellis-Davies, & Khodakhah, 2008).

In this thesis TBs and WBs were identified based on rate, using a “rebound index” (RI), defined as the maximum instantaneous firing rate (1/minimum interspike interval) divided by the cell’s baseline rate preceding hyperpolarization. Cells with RI >10 were categorized as TBs, and those with RI <10 as WBs. Out of 145 cells recorded, 50 were TBs and 95 were WBs (Figure 1B). 98.6% (143) of all DCN neurons had an RI>1, indicating that rebound-supporting conductances were widely expressed at some level. Several cells did not fire at rest, typical of a

subtype of glycinergic interneurons and were not included in RI calculations (Uusisaari & Knöpfel, 2010).

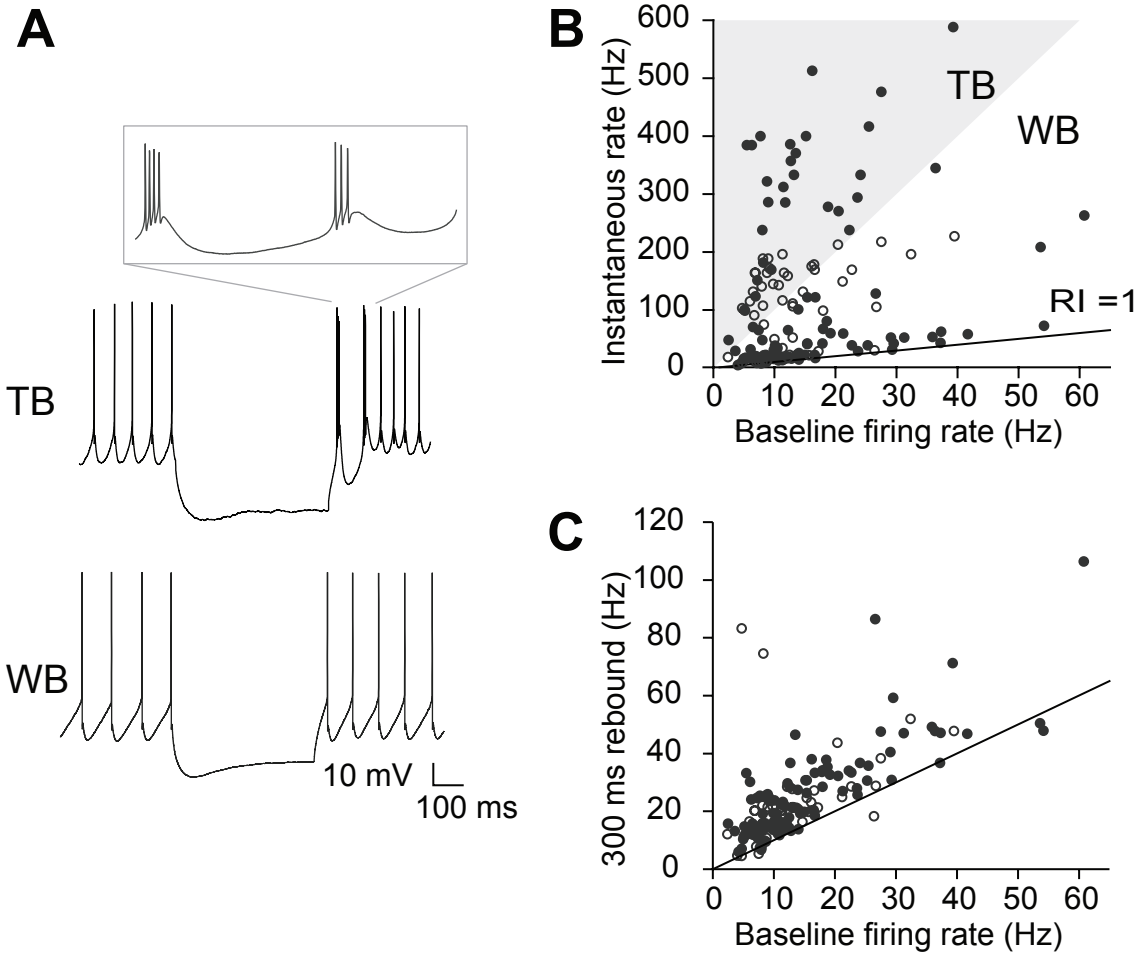


Figure 1. Definition of weak and transient bursters. A. Example voltage trace from a transient burster (TB) and weak burster (WB). Cells can be distinguished by their firing response to >500 ms hyperpolarization from I =0 to voltage near or below E_{Cl}. B. Maximum instantaneous firing rate (1/ISI) post-hyperpolarization vs. average baseline rate for cells recorded at 21˚C (∘) and 34˚C (•). Cells that lie within the shaded area (RI>10) are transient bursters. A unity line (—) is plotted for reference in B and C. C. Instantaneous firing rate (1/ISI) averaged over a 300 ms window following hyperpolarization vs. baseline firing rate.

Input resistance was 473.5 ± 367.5 (mean ± S.D.) in WBs and 395.9 ± 285.5 in TBs, consistent with values reported in the literature for large, primarily glutamatergic cells (Aizenman et al., 2003; Uusisaari et al., 2007). Previous reports suggest that WBs predominantly have small somata and dendritic arborizations (Czubayko et al., 2001) and thus would be expected to have higher input resistance than TBs. These results suggest that this population does not substantially contribute to our sample.

Instead of RI, rebound rate can be calculated from the instantaneous rate averaged over the first 300 ms following removal of hyperpolarization (Figure 1C). However, this quantity does not significantly differ between TBs and WBs at either temperature, suggesting that TBs don't generally more spikes than WBs in this interval but that the spike timing differs between these two cell classes.

Temperature-dependence of bursting behavior

To measure temperature-dependence of firing characteristics at lower temperatures, we compared baseline firing, post-hyperpolarization firing, and rebound characteristics in 22 TBs and 30 WBs at 21˚C, and 28 TBs and 64 WBs at 34˚C. At zero injected current, at 34˚C the average firing rate was higher (15.7 ± 10.9 Hz, range 2.5-60.8 Hz (mean ± S.D.), n=93; at 21˚C, 12.0 ± 7.4 Hz, range = 2.4-39.5 Hz, n= 52 cells; $p<0.02$, two-tailed t-test). Input resistance was comparable across temperature (425.5 ± 342.5 MΩ at 34˚C, 482.9 ± 341.6 MΩ at 21˚C). However, TBs had significantly lower input resistance at 34˚C than at 21˚C (TB, mean at 34˚C = 297.8 ± 206.8 MΩ, $p<0.01$).

Both post-hyperpolarization firing rate and rebound index (RI) were increased at higher temperatures. Post-rebound rate in WBs significantly differed from baseline at both temperatures

(34˚C, $p<10^{-4}$, n= 64; 21˚C, $p<10^{-3}$, n = 30). In TBs RI was significantly higher at 34˚C than at 21˚C (25.6 ± 15, n = 28 at 34˚C, 16.8 ± 5, n = 22, p<0.005, 2-tailed t-test). The maximum instantaneous firing rate following hyperpolarization was unchanged at 21˚C (101.4 ± 71 Hz, range 4.7 to 227.3 Hz) and 34˚C (121.8 ± 145 Hz, range 6 to 588 Hz). These measurements indicate that although TB and WB neurons are both found at high and low temperatures, the conductances that underlie rebound firing are substantially enhanced at higher temperatures.

Electrophysiological phenotype varies by anatomical location

Attempts to correlate bursting with electrophysiological and morphological parameters have been extensively studied in the literature with moderate success. Cells possessing the smallest somata and dendritic arbors, thought to be local interneurons, do not burst (Czubayko et al., 2001). For this reason we did not attempt to limit our observations to one cell type as defined by size or morphology. From the range of soma sizes, locations recorded and whole-cell parameters our results appear to come from a mixed population of neurons, primarily larger projection neurons that could have a glutamatergic or GABAergic phenotype (Aizenman et al., 2003; Uusisaari et al., 2007).

Instead we sought to determine differences as a function of location in the three deep nuclei, which receive input from distinct zones of the inferior olive and cerebellar cortex. Some evidence exists that each nucleus is functionally distinct in that cells within each nucleus receive input from different assembles of Purkinje cells in the cerebellar cortex and project to different regions (Buisseret-Delmas, Angaut, Compoint, Diagne, & Buisseret, 1998; Chan-Palay, 1977; Ruigrok & Voogd, 2000; Strick et al., 2009; Teune, van der Burg, van der Moer, Voogd, & Ruigrok, 2000). Turner and colleagues proposed that bursting occurred in a mediolateral

gradient, with a higher percentage of bursting neurons in the lateral nuclei (Tadayonnejad, Mehaffey, Anderson, & Turner, 2009). For this reason the location of a subset of cells within the deep nuclei were documented in order to assess whether there was systematic variation with location and bursting (Figure 2).

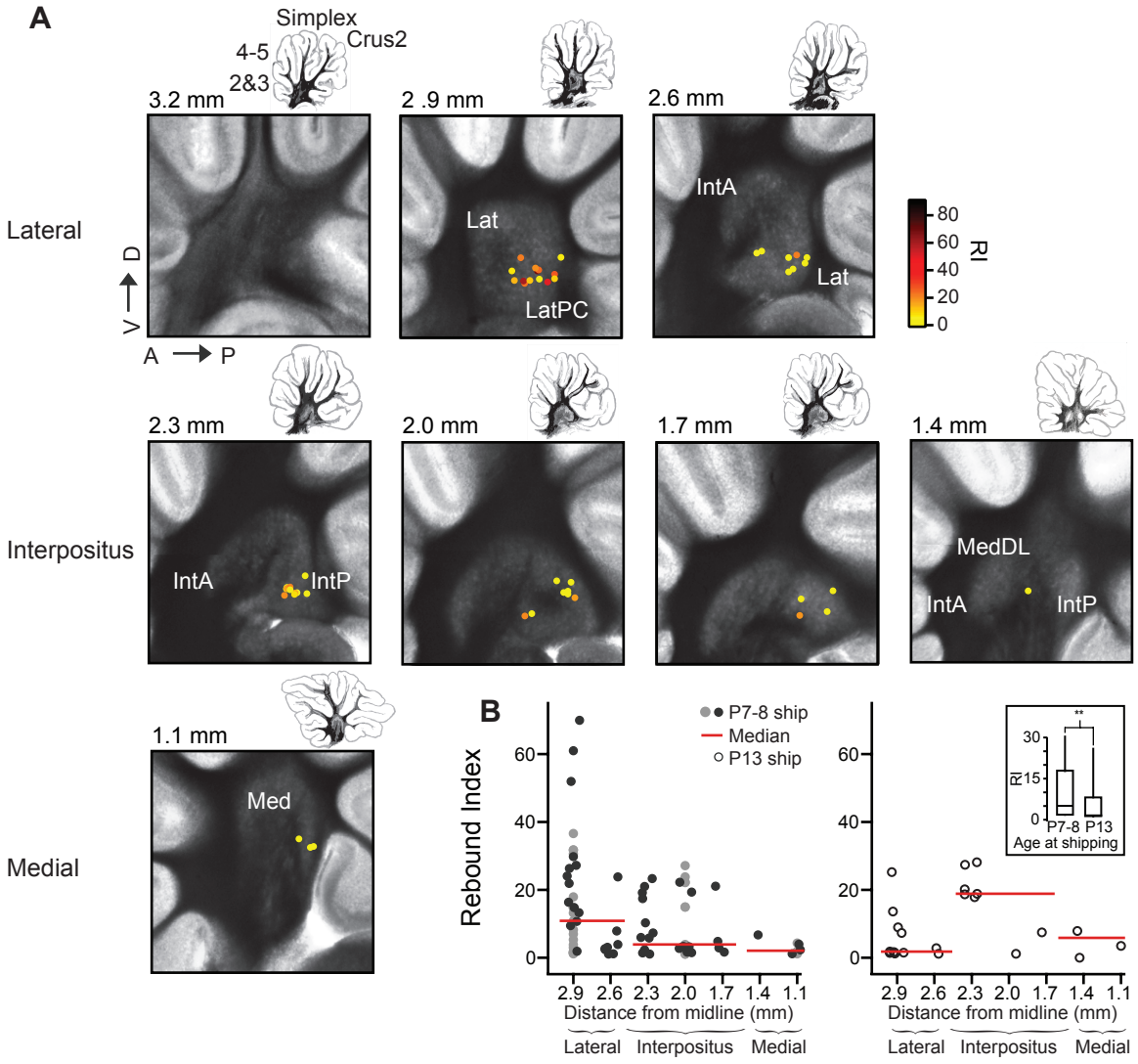


Figure 2. Location of weak and transient bursters. A. Location of cells recorded (•) superimposed on photographs of 300 µm sagittal sections of living DCN tissue. Sections are arranged from lateral to medial, left to right within each nucleus (Lateral, Interpositus, Medial). Rebound index (RI = mean(ISI)/min(ISI)) is indicated by colorscale. Drawings show the entire cerebellum at each plane of section. Labels DV and AP indicate the directions of the dorsal-ventral and anterior-posterior axis. Numbers indicate approximate distance of each section from Bregma in the medial-lateral plane according to Paxinos & Watson. Abbreviations: Lat- Lateral nucleus, Lat-PC Lateral nucleus Pars Compacta, IntA- Interpositus Anterior, Med- Medial nucleus, MedDL- Medial nucleus, Dorsolateral Protruberance. B. Rebound index plotted for each plane of section. Filled black circles (•) indicate recordings from animals shipped on P7-8 where the exact location was documented, filled gray circles (•) indicate only the nucleus was documented (Lat, Med or Int). Horizontal lines (—) indicate the median RI in each nucleus. C. Data for animals shipped on P12-P13 (∘) plotted as in B. Inset of C shows a box and whisker plot of RIs from recordings at 34˚C grouped by shipping date, ** $p < 0.01$, n = 55 P7-8, 26 P13.

Recordings were obtained from all three deep nuclei, primarily from the ventral portion of the lateral nucleus, the posterior interpositus and medial nucleus. The findings of Tadeyonnejad were confirmed in that the majority of TBs were found in the lateral nucleus. 53% (22/41) of cells located in the lateral nucleus were TBs, compared to 38% (14/36) in the interpositus and 0% (0/8) in the medial nucleus. The region of the lateral nucleus neurons most heavily sampled was the lateral nucleus *pars compacta*. In the interpositus nucleus cells were exclusively recorded in the posterior interpositus.

The probability of finding bursting neurons in any of the nuclei is quite varied in the literature, even when restricting observations to recordings from cells with large soma size in the lateral nucleus (Molineux et al., 2008; Zheng & Raman, 2009) suggesting there may be other factors that regulate bursting. One parameter that varied in our experiments was the amount of time animals spent in the facility before participating in experiments. To assess whether this was significantly related to the number of transient bursters RIs were compared from recordings in animals that were either shipped at age P7-8 and spent an average of 8.2 ± 1 days in the facility or arrived on P13 and spent an average of 2.2 ± 1 days in the facility. Cells analyzed were limited to recordings at 34˚C in order to limit any other sources of variability. Pooling data across all nuclei showed that there were significantly more TBs in the group that arrived younger and spent more days in the facility (Kolmogorov-Smirnov test, $p < 0.01$, $n = 55$ P7-8 shipped animals, 26 shipped at P13. In our findings and previous reports the lateral nucleus has been suggested to have the highest ration of TBs to WBs, and this was confirmed in our data at young shipping age. There were significantly more TBs in the lateral nucleus in recordings from animals shipped at P7-8 than those shipped at P12-13 (two-tailed t-test assuming unequal

variance, ($p < 0.005$, n = 54 cells, including 21˚C data) whereas this difference was not significant in the interposed and medial nuclei.

Because finding TBs was less likely under some experimental conditions, a subset of slices were pre-treated with the PKC activator phorbol-myristate-13-acetate (PMA) at 37˚C for 10 minutes before transferring the slice to the recording chamber. This compound has been shown to increase T-type calcium currents in several preparations, including thalamic reticular neurons (Chemin et al., 2007; Joksovic et al., 2010). PMA (200-400 nM) increased the probability of finding transient bursters. The fraction of transient bursters in PMA treated cells was significantly different than non-treated cells (10 TBs:14 PMA-treated cells vs 9 TBs: 67 non-treated cells, Fisher exact test, $p<0.0001$, Figure 3C). RIs, size and time-course of calcium transients in cells from PMA-treated slices were within the range of naturally occurring TBs, and three of these cells were included in subsequent pharmacology experiments.

The preponderance of TBs in the lateral and interpositus nuclei suggests that location within the nuclei can be used to locate transient bursters. Environmental factors can also play a role in the ability of cells to burst. So far our findings confirm reports in the literature that DCN neurons vary widely in their ability to produce rebound bursts. It is not yet known whether the same stimuli that cause neurons to burst also elicit dendritic calcium spikes, and whether these can occur both cell types or are exclusively limited to TBs.

DCN neurons have dendritic calcium spikes

The ability of DCN neurons to generate calcium entry has been a topic of interest since the first demonstration that DCN cells could undergo LTP. Hyperpolarizing steps can cause calcium entry in the soma and proximal dendrites during the rebound (Aizenman et al., 1998). Further, protocols that induce LTP also allow calcium entry in the soma and proximal dendrites (Pugh & Raman, 2008; Zheng & Raman, 2009). Repetitive burst stimuli that evoke plasticity of intrinsic excitability also generate calcium entry in both proximal and distal dendrites (Zhang et al., 2004).

To measure whether DCN neurons could produce dendritic calcium transients, and whether they were electrically regenerative, we performed two sets of experiments.

In the first experimental condition, cells were recorded at room temperature. To measure dendritic calcium transients cells were filled with 200 μM Calcium Green-1 for >40 minutes to visualize the dendrites. Cells were held at hyperpolarized potentials to prevent spiking, and then the hyperpolarization was briefly removed, allowing the cell to burst. Transients were measured at multiple points along the dendrites at distances between 20 and 122 μm from the soma. The mean fluorescence change during rebound in TBs was 81.6 ± 62.5 %ΔF/F (n = 9 cells, 68 measurements) whereas in WBs it was 103.6 ± 72.4 %ΔF/F (n = 5 cells, 38 measurements). To determine whether the calcium transients originating from WBs and TBs could belong to the same distribution a K-S test was performed. The two distributions were not significantly different. This led us to conclude that WBs and TBs are both capable of having large dendritic calcium transients.

To ensure that signals were not saturating, subsequent experiments were performed using the lower affinity calcium indicator dye fluo-5F (200 μM). These experiments were done at

using 8 line bandscans with a frame rate of 62.5 Hz at 34˚C to more accurately assess the amplitude and time-course of calcium transients. Cells were allowed to spike freely at I=0 and were then hyperpolarized for 1 second then returned to I=0. Peak change in fluorescence was calculated during the first 300 ms after the hyperpolarization was removed.

Qualitatively, cells showed varying amounts of dendritic calcium entry. On one extreme a subset of cells had very little calcium entry following hyperpolarization, barely overshooting the steady-state dendritic calcium (Figure 3A, B). As was the case for data collected at room temperature, the size of calcium transients in WBs and TBs did not significantly differ. Comparisons of peak calcium entry between the two groups were made at distances between 70 and 374 μm from the soma, following 1 second hyperpolarizations to voltages at or below E_{Ck}. The mean fluorescence change during rebound in TBs was 148.6 ± 87.4 and the interquartile range was 56.7-169.1 %ΔF/F (n=10 cells, 56 measurements). Often WBs had substantial dendritic calcium entry, comparable to many TBs (middle two sets of traces in Figure 3B). In WBs the average change in fluorescence was 97.5 ± 55.7, interquartile range: 56.7-125.1 % ΔF/F (n = 10 cells, 32 measurements). Dendritic spikes in TBs could be extremely large in amplitude (far left trace, Figure 3B), but on the whole the distribution of the size of calcium transients following hyperpolariation did not significantly differ between WBs and TBs.

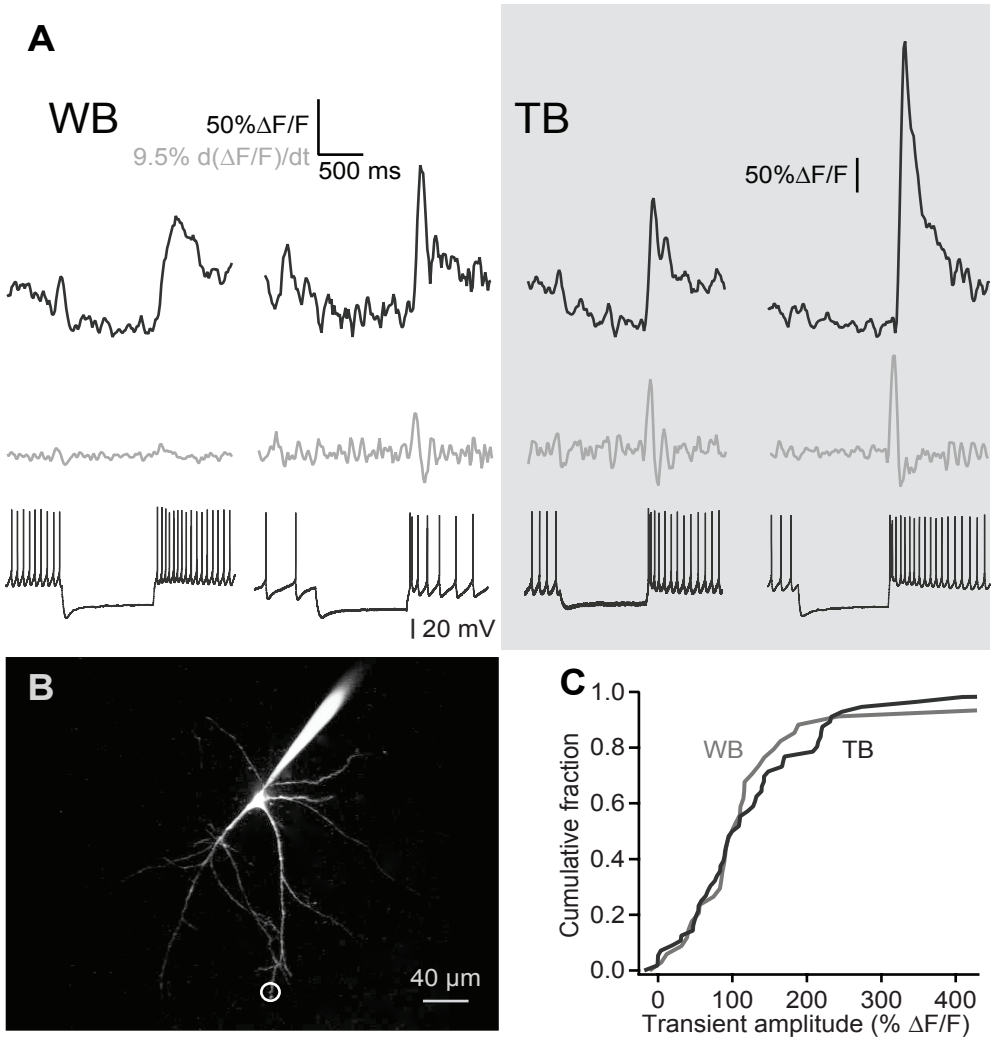


Figure 3: Example calcium signals from weak and transient bursters. A.Example calcium and voltage traces from two WB and TB neurons. Time derivatives of the calcium transient (—) and membrane voltage are shown below the calcium traces. B. Arborization patterns and recording locations from a typical DCN neuron, in this case the WB shown on the far left in panel A. C. Histogram of calcium transient peak amplitudes from 10 TBs (—) and 10 WBs (—) measured after hyperpolarizing steps ≤ ECl in dendrites 70-374 µm from the soma.

The kinetics of dendritic calcium entry differed in TBs and WBs. In TBs, the calcium transient was generally largest immediately following the removal of hyperpolarization, decaying rapidly back to steady-state calcium levels. This is particularly evident in the derivative of the calcium transient (Figure 3B, traces on right). In TBs and some WBs the derivative is largest immediately after the removal of hyperpolarization, suggesting the majority of the calcium flux occurs within the first 300 ms after hyperpolarization is removed. This is particularly of interest because it argues against the possibility that dendritic spikes are dependent on calcium entry associated with sodium spiking, as in this case dendritic calcium would slowly accrue with successive spike. Slowly rising time-courses can be seen in WBs with less calcium entry, but not in TBs (Figure 3B, trace on left). The size of the peak derivative was significantly different between TBs and WBs. In WBs the peak derivative of the calcium transient calculated from smoothed traces was 1.2 ± 0.7 ms whereas in TBs it was 2.2 ± 1.4 ms ($p < 0.0001$, KS test, n=10 TBs, 10 WBs). These results suggest that while both neuronal types are capable of producing calcium transients, they are faster in TBs. However, the source of calcium entry in DCN dendrites is not yet understood. It has been suggested that T-type calcium channels drive dendritic spikes, and the fast kinetics of calcium transients in TBs could reflect the higher expression of the Cav3.1 isoform in these neurons (Molineux et al., 2006). However, DCN neurons also have many L-type calcium conductances that could open in response to BAPs from the soma and studies of calcium entry in proximal dendrites have shown that calcium entry is highly correlated with firing rate (Zheng & Raman, 2009).

Dendritic calcium spikes require T-type channels but not sodium channels

We have shown thus far that DCN dendrites are capable of making large calcium spikes upon removal of hyperpolarization. Potential sources of calcium entry in DCN dendrites could be any of the wide variety of voltage-gated calcium channels DCN neurons express, primarily N, L and T/R. L-type calcium channels open in response to high voltages reached when the cell is spiking. It is likely that these channels are predominantly located on the soma, or uniformly distributed across cellular compartments (Zheng & Raman, 2009). In contrast, T-type calcium channels have been shown to be located on the dendrites as well as the soma (Molineux et al., 2006) and larger LVA currents are present in the dendrites (Gauck et al., 2001). These channels open at moderate voltages near spike threshold and are inactivated at high voltages. Current-clamp protocols such as ours that utilize a hyperpolarizing step to elicit a calcium spike allow for the removal of T-type inactivation, but if the cell is spiking during the rebound one cannot rule out the spike-associated calcium influx from L-type channels without pharmacological means.

If the dendritic calcium transients depend on LVA channels rather than the spike-associated influx of calcium through HVA channels, the calcium transients would be expected to persist even if spiking were blocked. To test this hypothesis we first blocked spiking using the sodium channel blocker tetrodotoxin (TTX) at concentrations ranging from 2-5μM. In Transient bursters (including one cell treated with PMA) calcium transients persisted in the presence of TTX and actually increased by 14.1 ± 58% on average (Figure 4.A, B). This confirms our hypothesis that spiking is not strictly necessary to drive dendritic calcium transients in TBs. The slight increase in the size of calcium transients can be explained by the fact that when spikes are blocked the mean voltage before hyperpolarization is lower than when cells are freely spiking, allowing partial removal of T-type channel inactivation. This further suggests that

hyperpolarizing voltage is a more critical determinate of bursting than firing rate. In WBs, the size of the transient dropped by 39.8 ± 31%. The effect of TTX was not statistically significant in either TBs or WBs (WBs: $p = 0.3$, $n = 4$; TBs: $p = 0.5$, $n = 7$). This suggests that in TBs the dendritic spike does not depend on back-propagating sodium spikes. In WBs, calcium transients are attenuated, but not blocked, suggesting calcium entry associated with spiking entry plays a larger role but does not account for the majority of the calcium influx.

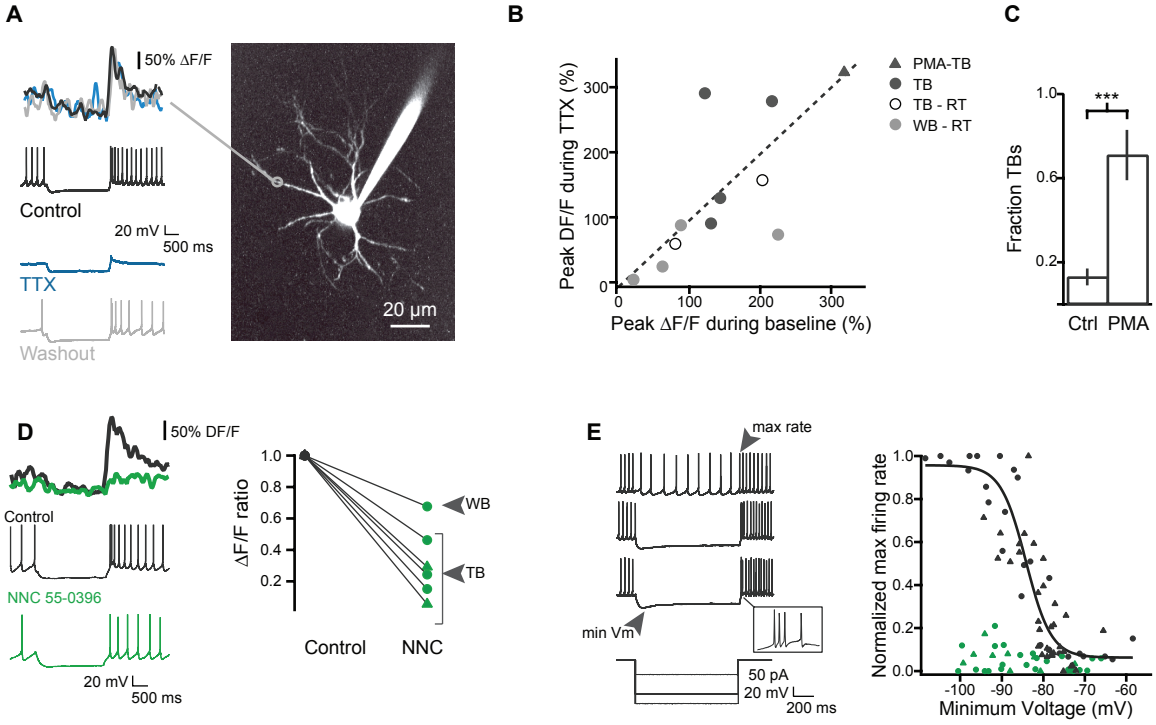


Figure 4: Pharmacology of dendritic calcium transients. A. Example transients and membrane voltage before (—), during (—) and after (—) application of 2 µM Tetrodotoxin (TTX) imaged at the dendritic location shown on the cell image. B. Graph showing the peak ΔF/F during TTX application (2-5 µM) in all cells tested vs. the peak ΔF/F before TTX. Symbols indicate whether cells were WBs or TBs recorded at 21˚C (RT) or 34˚C or treated with PMA to make it a transient burster before testing TTX. C. Number of transient bursters in animals shipped at P13 vs. the number of transient bursters in slices pretreated with 200-400 nM PMA. *** indicates $p<.0001$, KS test, n=67 cells without PMA treatment, 14 cells with PMA. Error bars are SD for a binomial distribution ($\sqrt{npq}$). D. Example traces before and after application of 10 µM NNC 55-0396. Graphon right shows the ratio of peak ΔF/F before NNC and after, showing it decreasedin all cells, particularly in TBs (●) and PMA-TBs (▲). E. Example of firing patterns elicited by successive steps of hyperpolarization before the application of NNC, showing the region for calculating the minimum voltage and maximum instantaneous rate used for the graph on right. Inset shows high-frequency burst at low Vm. In this graph firing rates in TBs were normalized either by the max and min rebound rates and fit by a sigmoid. The two PMA cells are not included in sigmoid fit.

In TBs dendritic calcium transients persisted in the presence of TTX, suggesting LVA calcium channels as the source of calcium entry. Because T-type calcium channels are suggested to be present at high densities in DCN dendrites (Molineux et al., 2006) and are necessary for generating rebound bursts (Alviña, Ellis-Davies, & Khodakhah, 2009) we chose to selectively block T-type calcium channels with NNC 55-0396 at 10-15 μM. At this dosage, NNC 55-0396 is thought to specifically block T-type calcium channels because the IC_{50} for T-type calcium current is 6.8 μM, whereas concentrations above 100 μM are needed to block HVA channels (Huang et al., 2004; Li, Hansen, Huang, Keyser, & Taylor, 2005). Cessation of bursting at voltages >95 mV was used as the criteria for beginning imaging experiments following drug application (Figure 4D, traces on left). In TBs the relationship between firing rate and voltage during the hyperpolarization can be fit by a sigmoid curve (Figure 4D). The mean normalized rate following hyperpolarizing steps ranging from -100 to -58 mV was 0.47 ± 0.38 (n=4 cells, 24 traces. After NNC 55-0396 treatment this decreased to 0.05 ± 0.05 (paired t-test n = 24, $p<0.0001$). In this respect our findings are similar to those reported in the literature (Alviña et al., 2009). In order to assess whether NNC 55-0396 would block dendritic calcium influx cells were imaged at several dendritic locations before and after application of the NNC 55-0396 (Figure 4C). Difference in peak amplitude of the calcium transient under baseline conditions and during NNC 55-0396 treatment was correlated with distance from the soma ($r = 0.41$, $n = 6$) and thus that comparing the effect of NNC across cells at different distances from the soma could be a confound. To avoid this, dendritic calcium transients were compared at the most distal locations imaged for each cell (111.5-317 μm, mean = 199.4 ± 50). NNC 55-0396 significantly reduced the size of dendritic calcium transients ($p < 0.001$, paired two-tailed t-test assuming equal variance, $n = 6$). At more proximal locations NNC 55-0396 was less effective at inhibiting

dendritic calcium entry, suggesting that calcium entering through HVA channels opened by the back-propagating action potential made a greater contribution at these locations.

In PMA-treated cells exposed to 15 μM NNC 55-0396 application of the drug transiently stopped the cells from spiking; suggesting either a nonspecific effect on sodium channels. This effect was not observed in non-PMA treated cells, or at the 10μM concentration, suggesting NNC 55-0396 has a nonspecific effect on sodium channels at higher concentrations. For instance, at 50μM NNC 55-0396 has been shown to block sodium channels (Fekete, A, Snutch, TP, & Delaney, KR, 2012). Because the cessation of spiking is a potential confound, imaging during NNC was not performed until spiking resumed, 15-55 minutes after NNC 55-0396 exposure. Since blockade of T-type calcium channels by NNC 55-0396 is not reversible (Li et al., 2005) the drug was not washed out.

From these results it follows that in neurons capable of producing dendritic calcium spikes, calcium influx depends more on T-type calcium channels more than calcium channels activated by sodium spikes. Additionally, T-type channel blockade is most efficacious at distal sites. This finding supports prior results in the literature that suggest dendritic calcium spikes could be larger with increasing distance from the soma (Aizenman et al., 1998; Gauck et al., 2001; Zhang et al., 2004).

Dendritic spikes are distal to the soma

In other neuronal types expressing T-type calcium channels calcium signals are larger on distal dendrites than proximal dendrites (Crandall et al., 2010; Johnston & Delaney, 2010). DCN neurons are also thought to express more T-type channels in dendrites than in the soma and peri-somatic regions (Molineux et al., 2006). Therefore DCN neurons may have larger calcium transients in distal dendrites than proximal dendrites. To assess this possibility we made multiple measurements from DCN neurons at distal and proximal locations.

Measurements were made using 8-line band scans at 62.5 Hz. Where possible the scanning axes were oriented to include proximal and distal regions in the same frame. In cases where this was not possible because the dendrites were insufficiently planar or the dendritic region was too distal and necessitated comparison of transients from separate scans, regions belonging to each dendrites were only compared where the minimum voltage were within 2.75 mV of each other (mean 0.8 ± 1mV) and the average voltage during hyperpolarization was within 2.23 mV across trials (mean = 0.5 ± 1mV). For example dendritic locations see Figure 5.A. In cases where the minimum hyperpolarization voltage differed by more than 1 mV the distal region was always the more depolarized of the two, to avoid biasing the data toward larger distal signals. The minimum voltage during hyperpolarization was -90.4 ± 10 mV. The average hyperpolarization was -82.9 ± 6 mV. Resting fluorescence (F) was calculated while the cell was freely spiking at I=0. The average fluorescence decrease during baseline spiking was -6.7 ± 14% ΔF/F, and decreased to -32.5 ± 18 %ΔF/F during the hyperpolarization (n = 9 cells, 24 regions). The minimum fluorescence change during the hyperpolarizing step was -49.3 ± 23 %ΔF/F. During rebound the peak fluorescence change increased to 125.9 ± 81 %ΔF/F. Path distance was calculated from z-stacks through cells using the soma center as the origin and the center of the

dendritic region scanned as the endpoint. Using this method distances ranged from 28 μm to 235 μm. Calcium transients across locations ranged from 9.28 to 348.5 % ΔF/F. Because of this large variation in the absolute size across cells data were normalized to the maximum ΔF/F within each dendrite (Figure 5. B). In WBs the normalized fluorescence change was significantly correlated with distance from the soma ($r = 0.82$, $p<0.001$, n = 13 locations, 6 dendrites). In TBs this correlation was not significant, as calcium transients are large even at proximal sites (n = $r = 0.21$, $p = 0.49$, 13 locations, 6 dendrites). At the most proximal locations measured (<100 μm) TBs had significantly larger calcium transients than WBs ($p<0.05$, n = 2 TBs, 4 WBs) whereas at more distal locations the populations did not significantly differ (Figure 5B). This suggests that there is greater expression of T-type conductances near the soma in TBs than in WBs, and this perhaps contributes to differences in rebound firing patterns among these neuronal populations.

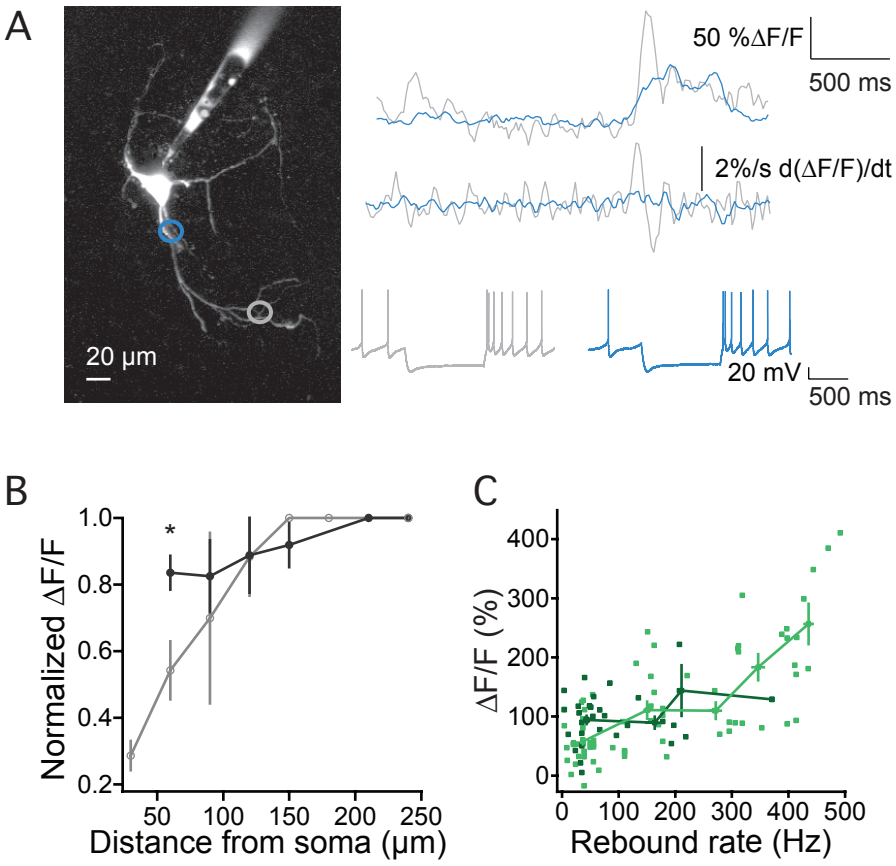


Figure 5: Calcium transients are larger distal to the soma. A. Example cell in which proximal (—) and distal (—) regions were imaged. Calcium transients, their derivatives and membrane voltage are shown on right. B. ΔF/F normalized to the maximum within-cell ΔF/F for 4 TBs (●) and 5 WBs (○) scanned at varying distance from the soma, averaged in 30 µm bins. C. Peak ΔF/F from 12 cells at proximal (■) and distal (■) locations vs. maximum instantaneous firing rate during rebound. Lines are averages binned at 50 Hz. Error bars in C and D are S.E.M.

Dendritic spikes are independent from firing rate at distal locations

That signals in distal regions tended to be larger than in proximal regions in weak bursters led us to question if at distal locations the size of the dendritic calcium spike was related to the firing rate at the soma. Near the soma dendritic calcium is highly correlated with average rebound rate, but it is not clear that this is the case at distal locations (Zheng & Raman, 2009). To test this hypothesis, dendrites were imaged during rebound from a range of hyperpolarizing voltages (from -101 to -53 mV average hyperpolarization) intended to elicit different amount of rebound bursting. Dendrites were imaged at distances between 28 and 317 μm. Under these conditions rebound rates ranged from 3.9 to 491.4 Hz (Figure 5C). Maximum instantaneous firing rate was well correlated with the size of the dendritic calcium transient at distances <140 μm from the soma ($r = 0.72$, $p < 10^{-6}$, $n = 71$ measurements, 7 cells). At more distal locations this correlation dropped to 0.23 and was not significant ($n = 30$ measurements, 4 cells). One cell that was only measured at proximal locations exhibited higher rebound rates (up to 491 Hz) and larger calcium spikes (410% $\Delta F/F$) than any of the cells measured at more distal points. In this cell rebound rate and peak $\Delta F/F$ were highly correlated ($r = 0.8$, $p<0.001$). The correlation between rebound and peak fluorescence at proximal locations remained significant without including measurements from this cell ($p<10^{-5}$, $n = 55$ measurements, 6 cells). The minimum hyperpolarization voltage showed a significant negative correlation with the size of the calcium transients at both proximal and distal locations ($r = -0.41$, $p < 0.02$ distal locations, $p<0.001$ proximal locations).

The observation that calcium transients at distal sites are independent of rebound rate, coupled with the finding that T-type blockade is more effective at distal sites leads to some interesting conclusions about the role of somatic spiking in distal dendrites. On the surface it

could seem that this could be the case because action potentials fail to propagate to distal regions. It is not yet known whether individual APs propagate into distal DCN dendrites. However it was clear that spiking does have an effect on dendritic calcium entry, and by extension, dendritic voltage. Steady-state calcium levels during tonic spiking were significantly different than the average fluorescence change during hyperpolarization at both distal and proximal regions ($p< 10^{-8}$ in both distal and proximal regions). This suggests that spiking does increase dendritic calcium entry. However, some of this decrease could be caused by a small T-type "window current" (Boehme, Uebele, Renger, & Pedroarena, 2011; Johnston & Delaney, 2010). However, because hyperpolarization is needed for large amounts of calcium influx through T-type channels for dendritic spikes the slight increase in dendritic calcium entry provided by HVA channels is of lesser importance to this phenomenon.

Dendritic calcium transients distal to the soma are not a function of decreasing dendrite diameter

The change in calcium concentration is a function of cytosolic volume and the soma and proximal regions have a larger volume than thinner dendrites. Calcium channels are located on the cell membrane. Dendrites with smaller diameters may appear to have larger calcium transients because of their large surface to volume ratio compared with peri-somatic regions. In order to test this hypothesis the diameter was measured from max projections of z-stacks taken after the recording. Diameters ranged from 1.24 to 6.19 μm with a mean value of 2.8 ± 1 μm (n = 11 cells, 26 measurements). Diameter did not significantly correlate with distance from the soma ($r = -0.31$, $n = 26$). This suggests that diameters did not differ enough between distal and

proximal regions to explain the correlation between peak fluorescence change and distance from the soma.

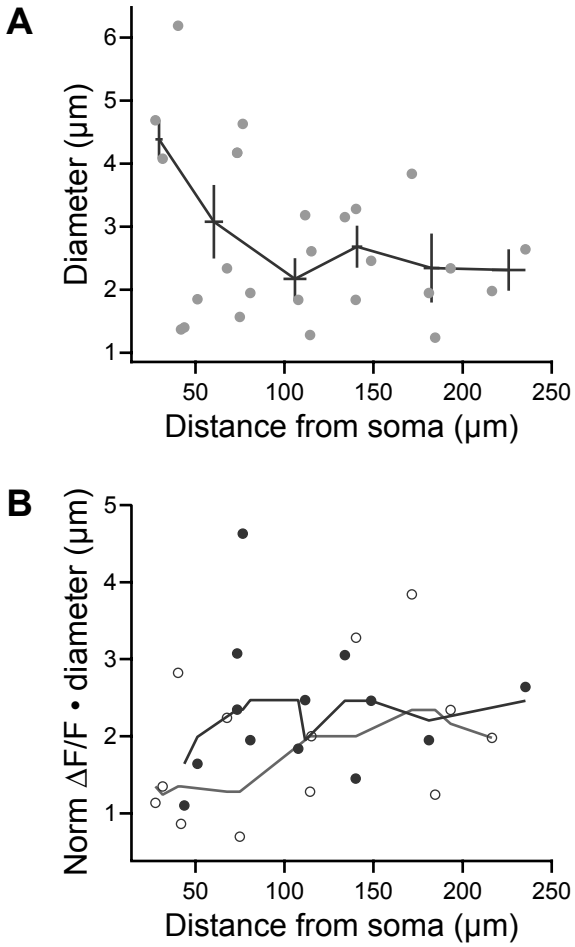


Figure 6. Distance dependence of calcium spikes is not a function of decreasing diameter. A. Diameter as a function of distance from the soma. Quantities plotted include raw data from combined TBs and WBs (•) and average values binned distance 40 µm (—). B. The product of normalized ΔF/F and diameter vs. distance from the soma. WBs are depicted by gray lines (—) and open circles ( ), TBs by black lines (—) and filled circles (•).

Taken as a whole the findings in this study suggest that DCN neurons are capable of producing large calcium transients. Neurons classified as TBs by their extremely high rebound firing rates have the largest and fastest calcium transients, though some WBs can also have comparable calcium transients. In WBs these transients are largest in the distal dendrites, whereas in TBs they are large throughout the dendrites. In TBs, these transients are driven by the T-type calcium channels as blocking these with the drug NNC 55-0396 significantly reduces the size of these transients. Sodium spiking does not drive dendritic calcium spikes, as blocking sodium channels with the drug TTX failed to significantly reduce the peak calcium transient in either cell type. Further, peak fluorescence change at distal locations is independent of rebound rate at the soma. The existence of dendritic calcium spikes in both cell types suggests they could play a role in dendritic integration, particularly at distal sites and possibly be a means of instructing plasticity at distal synapses.

Conclusions

Our results suggest that a mixed subset of DCN neurons have active dendrites, capable of producing large dendritic calcium transients. The size of dendritic calcium transients is proportional to the maximum instantaneous rate of somatic bursting at proximal locations on the dendrite, but in the distal dendrites calcium transients are independent of rebound rate. These finding confirms and extend previous results in the literature that alluded to the presence of dendritic spikes (Aizenman et al., 1998; Gauck et al., 2001; Zhang et al., 2004). Results in WBs are also consistent with the idea that proximal dendrites have less calcium entry under the same conditions (Zheng & Raman, 2009).

Previous studies show that blocking sodium channels blocks the high-frequency firing during rebound in TBs, but reveals an the underlying waveform of transient depolarization suggested to calcium influx through LVA channels (Aizenman & Linden, 1999; Llinás & Mühlethaler, 1988) and further studies confirm this (Alviña et al., 2009; Molineux et al., 2008). Our results show that dendritic spikes also persist despite sodium channel blockade. In both cell types over 50% of the calcium transient remained in the presence of TTX, and in TBs calcium transients fully persisted during TTX exposure. Further, the amplitude of calcium transients is much larger than can be predicted by the increase in number of spikes during rebound firing, suggesting it is not driven by spike-associated calcium influx through HVA channels. These results suggest sodium spikes are not necessary for dendritic calcium transients, whereas hyperpolarizing input is crucial for driving dendritic calcium spikes.

Hyperpolarizing input plays a major role in plasticity in DCN neurons. Of all the forms of plasticity that have been demonstrated in this region, there is not one that does not involve hyperpolarization in some way. One potential reason for this is that hyperpolarization is

necessary to prevent calcium influx through L-type calcium channels, a condition necessary for MF LTP (Person & Raman, 2010). Another reason, that is not mutually exclusive, is that it is necessary to drive dendritic calcium transients. In TBs, these calcium transients are generated by calcium influx through T-type channels, as evidenced by the robust blockade of these signals with the relatively specific T-type antagonist NNC 55-0396. This is also consistent with the idea that both TBs and WBs express T-type calcium channels (McKay et al., 2006; Molineux et al., 2006). Larger LVA currents in distal dendrites than the soma have been previously demonstrated (Gauck et al., 2001). Because of the use of the specific T-type channel NNC 55-0396, this is the first functional demonstration that the dendritic spike in distal dendrites is T-type in origin. This block is more effective at distal sites than proximal, providing further confirmation. While excitatory input alone can drive high firing rates and some calcium entry in the soma, only hyperpolarization can cause true dendritic spikes.

This is particularly of interest because of the dendritic location of excitatory synapses. Without dendritic calcium spikes it is possible that learning rules could be very different at proximal synapses and distal synapses. As stated previously hyperpolarization causes dendritic spikes and is necessary for plasticity. Rebound bursting can also be evoked *in vivo* by olivary stimulation and stimulation of the cerebellar cortex that mimics trains of simple or complex spikes (Bengtsson, Ekerot, & Jörntell, 2011; Hoebeek et al., 2010). In slices hyperpolarizations below the reversal potential for chloride (E_{Cl}) are sometimes required to elicit rebound bursts (Alviña et al., 2008; Zheng & Raman, 2009) and dendritic calcium influx (Zheng & Raman, 2009). This is relevant because the main inhibitory synaptic input to DCN neurons are Purkinje cells that release GABA, opening a chloride conductance to hyperpolarize DCN cells and thus cannot go below E_{Cl}. However, rebound bursting can be evoked in slices by GABA uncaging,

which by definition does not hyperpolarize below E_{Cl} (Alviña et al., 2009). Further, a fraction of maximal T-type calcium current is available even during very brief hyperpolarization above E_{Cl} (Engbers et al., 2011). There are several reasons as to why rebound can be so reliably evoked *in vivo* as opposed to in slices. Because of the geometry of inputs, in slices it may be difficult to stimulate the full array of convergent PC inputs to a DCN neuron with one electrode. This may be accomplished *in vivo* by synchronous activation of many climbing fibers. Further, CF stimulation could provide both the sequence of coincident inhibition and excitation, followed by disinhibition necessary for MF LTP. It is established that climbing fiber synchrony occurs in awake behaving animals in the cerebellum (Ozden, Dombeck, Hoogland, Tank, & Wang, 2012).

Another reason bursting might be more prevalent *in vivo* is that neuromodulatory tone may be present in the DCN *in vivo* that is not present in slice. The DCN is known to receive ample neuromodulatory input (Chan-Palay, 1977; Dieudonné, 2001; Jaarsma et al., 1997) and there have been reports of neuromodulator receptors coupling to T-type channels and increasing or decreasing the availability of T-type channels in other brain regions (Hildebrand et al., 2007; Hildebrand et al., 2009; Johnston & Delaney, 2010). Further, T-type channels form signaling complexes with Kv4 potassium channels that modulate firing rates and the efficiency of action potential back-propagation (Anderson et al., 2010).

PKC and PKA have both been shown to directly interact with T-type channels, both in culture and *in vitro* (Chemin et al., 2007; Joksovic et al., 2010). In our experiments this was used to increase the probability of finding neurons that behaved like TBs. This suggests the intriguing possibility that neurons exhibit TB or WB phenotypes depending on the availability of T-type channels. Future experiments would be necessary to conclusively test this possibility. If the dendrites shift from a normal state to an active state by T-type channel phosphorylation, then

perhaps the relevant question is not *if* there are active dendrites in the DCN but *when* are the dendrites active, and *why*? What is the function of these calcium transients?

Regarding "why," there are several tantalizing hypotheses. One is that dendritic calcium signals could be instructive signals for plasticity. Plasticity in the DCN is necessary for learning in cerebellar behaviors (Krupa & Thompson, 1997; McCormick & Thompson, 1984; McCormick et al., 1982; McCormick, Guyer, & Thompson, 1982; Ohyama, Nores, & Mauk, 2003; Ohyama, Nores, Medina, Riusech, & Mauk, 2006) (Gruart, Blázquez, Pastor, & Delgado-García, 1994; Racine, Wilson, Gingell, & Sunderland, 1986). Conditions which produce LTP of synapses on DCN neurons are often permissive for generating dendritic calcium spikes (Aizenman et al., 1998; Pugh & Raman, 2008). This is also the case for protocols that increase intrinsic excitability in DCN neurons (Zhang et al., 2004). Further, firing patterns *in vivo* also suggest that dendritic calcium spikes may be generated under conditions not previously recognized. Activating the CF pathway generates rebound bursts in DCN neurons (Bengtsson et al., 2011; Hoebeek et al., 2010) which we have shown that rebound bursts are correlated with dendritic calcium spikes, particularly at proximal locations. Activating the climbing fiber is necessary for cerebellar learning, such as eye-blink conditioning, where direct stimulation of the inferior olive can substitute for the tone stimulus in this classic paradigm (Mauk, Steinmetz, & Thompson, 1986).

Dendritic spikes also provide a means to explain potentiation of distal inputs (Sjöström et al., 2008) or a mechanism for local amplification. Apart from their potential role in synaptic plasticity, dendritic calcium spikes can also have profound effects on the integration of synaptic input. For instance, in pyramidal cells and thalamic reticular neurons, even small synapses that arrive on very distal sites of the dendritic tree can trigger calcium spikes, resulting in a larger

change in somatic spiking than synapses of comparable strength at more proximal locations (Crandall et al., 2010; Williams & Stuart, 2002). Inputs to DCN neurons are distributed throughout the soma and dendrites, with the majority of excitatory inputs arriving on the dendrites (Chan-Palay, 1973a). The existence of dendritic calcium channels, and their ability to fire dendritic action potentials could alter the relative filtering of inputs that arrive at different distances on the dendrites, with consequences for the timing of spike output in DCN neurons, and local summation of synaptic inputs. How these factors orchestrate to control firing dynamics and dendritic integration in the DCN remains a rich area for future study.

Bibliography

Abbott, L. F., & Nelson, S. B. (2000). Synaptic plasticity: Taming the beast. ***Nature Neuroscience, 3 Suppl,*** **1178-83. doi:10.1038/81453**

Aizenman, C. D., & Linden, D. J. (1999). Regulation of the rebound depolarization and spontaneous firing patterns of deep nuclear neurons in slices of rat cerebellum. ***Journal of Neurophysiology, 82*****(4), 1697-709.**

Aizenman, C. D., Huang, E. J., & Linden, D. J. (2003). Morphological correlates of intrinsic electrical excitability in neurons of the deep cerebellar nuclei. ***Journal of Neurophysiology, 89*****(4), 1738-47. doi:10.1152/jn.01043.2002**

Aizenman, C. D., Huang, E. J., Manis, P. B., & Linden, D. J. (2000). Use-Dependent changes in synaptic strength at the purkinje cell to deep nuclear synapse. ***Progress in Brain Research, 124,*** **257-73.**

Aizenman, C. D., Manis, P. B., & Linden, D. J. (1998). Polarity of long-term synaptic gain change is related to postsynaptic spike firing at a cerebellar inhibitory synapse. ***Neuron, 21*****(4), 827-35.**

Alviña, K., Ellis-Davies, G., & Khodakhah, K. (2009). T-Type calcium channels mediate rebound firing in intact deep cerebellar neurons. ***Neuroscience, 158*****(2), 635-41. doi:10.1016/j.neuroscience.2008.09.052**

Alviña, K., Walter, J. T., Kohn, A., Ellis-Davies, G., & Khodakhah, K. (2008). Questioning the role of rebound firing in the cerebellum. ***Nature Neuroscience, 11*****(11), 1256-8. doi:10.1038/nn.2195**

Anchisi, D., Scelfo, B., & Tempia, F. (2001). Postsynaptic currents in deep cerebellar nuclei. ***Journal of Neurophysiology, 85*****(1), 323-31. doi:11152732**

Anderson, D., Rehak, R., Hameed, S., Mehaffey, W. H., Zamponi, G. W., & Turner, R. W. (2010). Regulation of the KV4.2 complex by cav3.1 calcium channels. ***Channels (Austin, Tex.), 4*****(3), 163-7.**

Bengtsson, F., Ekerot, C. F., & Jörntell, H. (2011). In vivo analysis of inhibitory synaptic inputs and rebounds in deep cerebellar nuclear neurons. ***Plos One, 6*****(4), e18822. doi:10.1371/journal.pone.0018822**

Berger, A., Sadeh, M., Tzur, G., Shuper, I. A., Kornreich, L., Inbar, D., . . . Vakil, E. (2005). Motor and non-motor sequence learning in children and adolescents with cerebellar damage. ***Journal of the International Neuropsychological Society : JINS, 11*****(4), 482-7. doi:16209429**

Berthier, N. E., & Moore, J. W. (1990). Activity of deep cerebellar nuclear cells during classical conditioning of nictitating membrane extension in rabbits. ***Experimental Brain Research. Experimentelle Hirnforschung. Expérimentation Cérébrale, 83*****(1), 44-54. doi:2073949**

Bischofberger, J., & Jonas, P. (1997). Action potential propagation into the presynaptic dendrites of rat mitral cells. ***The Journal of Physiology, 504 (Pt 2),*** **359-65.**

Bolduc, M. E., du Plessis, A. J., Sullivan, N., Guizard, N., Zhang, X., Robertson, R. L., & Limperopoulos, C. (2012). Regional cerebellar volumes predict functional outcome in children with cerebellar malformations. ***Cerebellum (London, England), 11*****(2), 531-42. doi:10.1007/s12311-011-0312-z**

Calderon, D. P., Fremont, R., Kraenzlin, F., & Khodakhah, K. (2011). The neural substrates of rapid-onset dystonia-parkinsonism. ***Nature Neuroscience, 14*****(3), 357-65. doi:10.1038/nn.2753**

Carulli, D., Rhodes, K. E., Brown, D. J., Bonnert, T. P., Pollack, S. J., Oliver, K., . . . Fawcett, J. W. (2006). Composition of perineuronal nets in the adult rat cerebellum and the cellular origin of their components. *The Journal of Comparative Neurology, 494*(4), 559-77. doi:10.1002/cne.20822

Chan-Palay, V. (1973a). Afferent axons and their relations with neurons in the nucleus lateralis of the cerebellum: A light microscopic study. *Zeitschrift Für Anatomie Und Entwicklungsgeschichte, 142*(1), 1-21.

Chan-Palay, V. (1973b). On the identification of the afferent axon terminals in the nucleus lateralis of the cerebellum. An electron microscope study. *Zeitschrift Für Anatomie Und Entwicklungsgeschichte, 142*(2), 149-86.

Chan-Palay, V. (1977). Cerebellar dentate nucleus. *Organization, Cytology and Transmitters.*

Chemin, J., Mezghrani, A., Bidaud, I., Dupasquier, S., Marger, F., Barrère, C., . . . Lory, P. (2007). Temperature-Dependent modulation of cav3 t-type calcium channels by protein kinases C and A in mammalian cells. *The Journal of Biological Chemistry, 282*(45), 32710-8. doi:10.1074/jbc.M702746200

Choi, J. S., & Moore, J. W. (2003). Cerebellar neuronal activity expresses the complex topography of conditioned eyeblink responses. *Behavioral Neuroscience, 117*(6), 1211-9. doi:10.1037/0735-7044.117.6.1211

Contreras, D., Curró Dossi, R., & Steriade, M. (1993). Electrophysiological properties of cat reticular thalamic neurones in vivo. *The Journal of Physiology, 470*, 273-94.

Courchesne, E., Townsend, J., Akshoomoff, N. A., Saitoh, O., Yeung-Courchesne, R., Lincoln, A. J., . . . Lau, L. (1994). Impairment in shifting attention in autistic and cerebellar patients. *Behavioral Neuroscience, 108*(5), 848.

Crandall, S. R., Govindaiah, G., & Cox, C. L. (2010). Low-Threshold ca2+ current amplifies distal dendritic signaling in thalamic reticular neurons. *The Journal of Neuroscience : The Official Journal of the Society for Neuroscience, 30*(46), 15419-29. doi:10.1523/JNEUROSCI.3636-10.2010

Czubayko, U., Sultan, F., Thier, P., & Schwarz, C. (2001). Two types of neurons in the rat cerebellar nuclei as distinguished by membrane potentials and intracellular fillings. *Journal of Neurophysiology, 85*(5), 2017-29.

Davie, J. T., Clark, B. A., & Häusser, M. (2008). The origin of the complex spike in cerebellar purkinje cells. *The Journal of Neuroscience : The Official Journal of the Society for Neuroscience, 28*(30), 7599-609. doi:10.1523/JNEUROSCI.0559-08.2008

Delgado-García, J. M., & Gruart, A. (2005). Firing activities of identified posterior interpositus nucleus neurons during associative learning in behaving cats. *Brain Res Brain Res Rev, 49*(2), 367-76. doi:10.1016/j.brainresrev.2004.10.006

Desmond, J. E., Gabrieli, J. D., & Glover, G. H. (1998). Dissociation of frontal and cerebellar activity in a cognitive task: Evidence for a distinction between selection and search. *Neuroimage, 7*(4 Pt 1), 368-76. doi:10.1006/nimg.1998.0340

Dieudonné, S. (2001). Serotonergic neuromodulation in the cerebellar cortex: Cellular, synaptic, and molecular basis. *The Neuroscientist : A Review Journal Bringing Neurobiology, Neurology and Psychiatry, 7*(3), 207-19.

Drepper, J., Timmann, D., Kolb, F. P., & Diener, H. C. (1999). Non-Motor associative learning in patients with isolated degenerative cerebellar disease. *Brain : A Journal of Neurology, 122 (Pt 1)*, 87-97.

Engbers, J. D., Anderson, D., Tadayonnejad, R., Mehaffey, W. H., Molineux, M. L., & Turner, R. W. (2011). Distinct roles for I(T) and I(H) in controlling the frequency and timing of rebound spike responses. *The Journal of Physiology, 589*(Pt 22), 5391-413. doi:10.1113/jphysiol.2011.215632

Ferrier, David (M.D.). (1886). *Functions of the brain.* London: Smith, Elder.

Fiez, J. A., Petersen, S. E., Cheney, M. K., & Raichle, M. E. (1992). Impaired non-motor learning and error detection associated with cerebellar damage. A single case study. *Brain : A Journal of Neurology, 115 Pt 1*, 155-78.

Freeman, J. H., & Nicholson, D. A. (1999). Neuronal activity in the cerebellar interpositus and lateral pontine nuclei during inhibitory classical conditioning of the eyeblink response. *Brain Research, 833*(2), 225-33.

Gardette, R., Debono, M., Dupont, J. L., & Crepel, F. (1985). Electrophysiological studies on the postnatal development of intracerebellar nuclei neurons in rat cerebellar slices maintained in vitro. I. Postsynaptic potentials. *Brain Research, 351*(1), 47-55.

Gauck, V., Thomann, M., Jaeger, D., & Borst, A. (2001). Spatial distribution of low- and high-voltage-activated calcium currents in neurons of the deep cerebellar nuclei. *The Journal of Neuroscience : The Official Journal of the Society for Neuroscience, 21*(15), RC158.

Gerlai, R., Millen, K. J., Herrup, K., Fabien, K., Joyner, A. L., & Roder, J. (1996). Impaired motor learning performance in cerebellar en-2 mutant mice. *Behavioral Neuroscience, 110*(1), 126-33.

Glickstein, M., Strata, P., & Voogd, J. (2009). Cerebellum: History. *Neuroscience, 162*(3), 549-59. doi:10.1016/j.neuroscience.2009.02.054

Golding, N. L., Kath, W. L., & Spruston, N. (2001). Dichotomy of action-potential backpropagation in CA1 pyramidal neuron dendrites. *Journal of Neurophysiology, 86*(6), 2998-3010.

Gruart, A., Blázquez, P., Pastor, A. M., & Delgado-García, J. M. (1994). Very short-term potentiation of climbing fiber effects on deep cerebellar nuclei neurons by conditioning stimulation of mossy fiber afferents. *Experimental Brain Research. Experimentelle Hirnforschung. Expérimentation Cérébrale, 101*(1), 173-7.

Häusser, M., Stuart, G., Racca, C., & Sakmann, B. (1995). Axonal initiation and active dendritic propagation of action potentials in substantia nigra neurons. *Neuron, 15*(3), 637-47.

Hildebrand, M. E., David, L. S., Hamid, J., Mulatz, K., Garcia, E., Zamponi, G. W., & Snutch, T. P. (2007). Selective inhibition of cav3.3 t-type calcium channels by galphaq/11-coupled muscarinic acetylcholine receptors. *The Journal of Biological Chemistry, 282*(29), 21043-55. doi:10.1074/jbc.M611809200

Hildebrand, M. E., Isope, P., Miyazaki, T., Nakaya, T., Garcia, E., Feltz, A., . . . Snutch, T. P. (2009). Functional coupling between mglur1 and cav3.1 t-type calcium channels contributes to parallel fiber-induced fast calcium signaling within purkinje cell dendritic spines. *The Journal of Neuroscience : The Official Journal of the Society for Neuroscience, 29*(31), 9668-82. doi:10.1523/JNEUROSCI.0362-09.2009

Hoebeek, F. E., Witter, L., Ruigrok, T. J., & De Zeeuw, C. I. (2010). Differential olivo-cerebellar cortical control of rebound activity in the cerebellar nuclei. *Proceedings of the National Academy of Sciences of the United States of America, 107*(18), 8410-5. doi:10.1073/pnas.0907118107

Holmes, G. (1917). The symptoms of acute cerebellar injuries due to gunshot injuries. *Brain : A Journal of Neurology*, *40*(4), 461.
Holmes Gordon. (1939). The cerebellum of man. *Brain : A Journal of Neurology*, *62*, 1-30.
Jaarsma, D., Ruigrok, T. J., Caffé, R., Cozzari, C., Levey, A. I., Mugnaini, E., & Voogd, J. (1997). Cholinergic innervation and receptors in the cerebellum. *Progress in Brain Research*, *114*, 67-96.
Jack, J. J. B., Noble, D., & Tsien, R. W. (1983). *Electric current flow in excitable cells.* Oxford: Clarendon Press.
Jahnsen, H. (1986). Electrophysiological characteristics of neurones in the guinea-pig deep cerebellar nuclei in vitro. *The Journal of Physiology*, *372*, 129-47.
Johnston, J., & Delaney, K. R. (2010). Synaptic activation of t-type ca2+ channels via mglur activation in the primary dendrite of mitral cells. *Journal of Neurophysiology*, *103*(5), 2557-69. doi:10.1152/jn.00796.2009
Joksovic, P. M., Choe, W. J., Nelson, M. T., Orestes, P., Brimelow, B. C., & Todorovic, S. M. (2010). Mechanisms of inhibition of t-type calcium current in the reticular thalamic neurons by 1-octanol: Implication of the protein kinase C pathway. *Molecular Pharmacology*, *77*(1), 87-94. doi:10.1124/mol.109.059931
Joyal, C. C., Pennanen, C., Tiihonen, E., Laakso, M. P., Tiihonen, J., & Aronen, H. J. (2004). MRI volumetry of the vermis and the cerebellar hemispheres in men with schizophrenia. *Psychiatry Research*, *131*(2), 115-24. doi:10.1016/j.pscychresns.2003.09.003
Kalmbach, B. E., Davis, T., Ohyama, T., Riusech, F., Nores, W. L., & Mauk, M. D. (2010). Cerebellar cortex contributions to the expression and timing of conditioned eyelid responses. *Journal of Neurophysiology*, *103*(4), 2039-49. doi:10.1152/jn.00033.2010
Klin, A., Lin, D. J., Gorrindo, P., Ramsay, G., & Jones, W. (2009). Two-Year-Olds with autism orient to non-social contingencies rather than biological motion. *Nature*, *459*(7244), 257-261.
Klockgether, T., & Paulson, H. (2011). Milestones in ataxia. *Mov Disord*, *26*(6), 1134-41. doi:10.1002/mds.23559
Krupa, D. J., & Thompson, R. F. (1997). Reversible inactivation of the cerebellar interpositus nucleus completely prevents acquisition of the classically conditioned eye-blink response. *Learning & Memory (Cold Spring Harbor, N.Y.)*, *3*(6), 545-56.
Krupa David J, Thompson Judith K Thompson Richard F. (1993). Localization of a memory trace in the mammalian brain. *Science (New York, N.Y.)*, *260*(5110), 989-991.
LeDoux, M. S., Hurst, D. C., & Lorden, J. F. (1998). Single-Unit activity of cerebellar nuclear cells in the awake genetically dystonic rat. *Neuroscience*, *86*(2), 533-45. doi:9881867
Levisohn, L., Cronin-Golomb, A., & Schmahmann, J. D. (2000). Neuropsychological consequences of cerebellar tumour resection in children: Cerebellar cognitive affective syndrome in a paediatric population. *Brain : A Journal of Neurology*, *123 (Pt 5)*, 1041-50. doi:10775548
Llinás, R., & Mühlethaler, M. (1988). Electrophysiology of guinea-pig cerebellar nuclear cells in the in vitro brain stem-cerebellar preparation. *The Journal of Physiology*, *404*(1), 241.
Llinás, R., & Sugimori, M. (1980). Electrophysiological properties of in vitro purkinje cell dendrites in mammalian cerebellar slices. *The Journal of Physiology*, *305*, 197-213.

Magee, J. C., & Cook, E. P. (2000). Somatic EPSP amplitude is independent of synapse location in hippocampal pyramidal neurons. ***Nature Neuroscience, 3*****(9), 895-903. doi:10.1038/78800**
Magee, J. C., & Johnston, D. (1997). A synaptically controlled, associative signal for hebbian plasticity in hippocampal neurons. ***Science, 275*****(5297), 209-13.**
Marsaglia G, Tsang WW, Wang J. (2003). Evaluating kolmogorov's distribution . *Journal of Statistical Software, 8*(18), 1-4. Retrieved from http://www.jstatsoft.org/v08/i18

Matilla-Dueñas, A. (2012). The ever expanding spinocerebellar ataxias. Editorial. ***Cerebellum (London, England).*** **doi:10.1007/s12311-012-0376-4**
Mauk, M. D., Steinmetz, J. E., & Thompson, R. F. (1986). Classical conditioning using stimulation of the inferior olive as the unconditioned stimulus. ***Proceedings of the National Academy of Sciences of the United States of America, 83*****(14), 5349-53. doi:3460097**
McAlonan, K., Cavanaugh, J., & Wurtz, R. H. (2006). Attentional modulation of thalamic reticular neurons. ***The Journal of Neuroscience : The Official Journal of the Society for Neuroscience, 26*****(16), 4444-50. doi:10.1523/JNEUROSCI.5602-05.2006**
McAlonan, K., Cavanaugh, J., & Wurtz, R. H. (2008). Guarding the gateway to cortex with attention in visual thalamus. ***Nature, 456*****(7220), 391-4. doi:10.1038/nature07382**
McCormick, D. A., & Thompson, R. F. (1984). Neuronal responses of the rabbit cerebellum during acquisition and performance of a classically conditioned nictitating membrane-eyelid response. ***The Journal of Neuroscience : The Official Journal of the Society for Neuroscience, 4*****(11), 2811-22.**
McCormick, D. A., Clark, G. A., Lavond, D. G., & Thompson, R. F. (1982). Initial localization of the memory trace for a basic form of learning. ***Proceedings of the National Academy of Sciences of the United States of America, 79*****(8), 2731-5.**
McCormick, D. A., Guyer, P. E., & Thompson, R. F. (1982). Superior cerebellar peduncle lesions selectively abolish the ipsilateral classically conditioned nictitating membrane/eyelid response of the rabbit. ***Brain Research, 244*****(2), 347-50.**
McKay, B. E., McRory, J. E., Molineux, M. L., Hamid, J., Snutch, T. P., Zamponi, G. W., & Turner, R. W. (2006). Ca(V)3 t-type calcium channel isoforms differentially distribute to somatic and dendritic compartments in rat central neurons. ***The European Journal of Neuroscience, 24*****(9), 2581-94. doi:10.1111/j.1460-9568.2006.05136.x**
Medina, J. F. (2011). The multiple roles of purkinje cells in sensori-motor calibration: To predict, teach and command. ***Current Opinion in Neurobiology, 21*****(4), 616-22. doi:10.1016/j.conb.2011.05.025**
Mel, B. W. (1993). Synaptic integration in an excitable dendritic tree. ***Journal of Neurophysiology, 70*****(3), 1086-101.**
Mel, B. W. (2002). Have we been hebbing down the wrong path? ***Neuron, 34*****(2), 175-7.**
Middleton, F. A., & Strick, P. L. (2001). Cerebellar projections to the prefrontal cortex of the primate. ***The Journal of Neuroscience : The Official Journal of the Society for Neuroscience, 21*****(2), 700-12. doi:11160449**
Molineux, M. L., McRory, J. E., McKay, B. E., Hamid, J., Mehaffey, W. H., Rehak, R., . . . Turner, R. W. (2006). Specific t-type calcium channel isoforms are associated with distinct burst phenotypes in deep cerebellar nuclear neurons. ***Proceedings of the National Academy of Sciences of the United States of America, 103*****(14), 5555-60. doi:10.1073/pnas.0601261103**

Molineux, M. L., Mehaffey, W. H., Tadayonnejad, R., Anderson, D., Tennent, A. F., & Turner, R. W. (2008). Ionic factors governing rebound burst phenotype in rat deep cerebellar neurons. ***Journal of Neurophysiology, 100*****(5), 2684-701. doi:10.1152/jn.90427.2008**

Murdoch, B. E. (2010). The cerebellum and language: Historical perspective and review. ***Cortex; A Journal Devoted to the Study of the Nervous System and Behavior, 46*****(7), 858-68. doi:10.1016/j.cortex.2009.07.018**

Neychev, V. K., Fan, X., Mitev, V. I., Hess, E. J., & Jinnah, H. A. (2008). The basal ganglia and cerebellum interact in the expression of dystonic movement. ***Brain : A Journal of Neurology, 131*****(Pt 9), 2499-509. doi:10.1093/brain/awn168**

Nicholson, D. A., & Freeman, J. H. (2002). Neuronal correlates of conditioned inhibition of the eyeblink response in the anterior interpositus nucleus. ***Behavioral Neuroscience, 116*****(1), 22-36.**

Ohyama, T., & Mauk, M. (2001). Latent acquisition of timed responses in cerebellar cortex. ***The Journal of Neuroscience : The Official Journal of the Society for Neuroscience, 21*****(2), 682-90. doi:11160447**

Ohyama, T., Nores, W. L., & Mauk, M. D. (2003). Stimulus generalization of conditioned eyelid responses produced without cerebellar cortex: Implications for plasticity in the cerebellar nuclei. ***Learning & Memory (Cold Spring Harbor, N.Y.), 10*****(5), 346-54. doi:10.1101/lm.67103**

Ohyama, T., Nores, W. L., Medina, J. F., Riusech, F. A., & Mauk, M. D. (2006). Learning-Induced plasticity in deep cerebellar nucleus. ***The Journal of Neuroscience : The Official Journal of the Society for Neuroscience, 26*****(49), 12656-63. doi:10.1523/JNEUROSCI.4023-06.2006**

Ozden, I., Dombeck, D. A., Hoogland, T. M., Tank, D. W., & Wang, S. S. (2012). Widespread state-dependent shifts in cerebellar activity in locomoting mice. ***Plos One, 7*****(8), e42650. doi:10.1371/journal.pone.0042650**

Ozden, I., Sullivan, M. R., Lee, H. M., & Wang, S. S. H. (2009). Reliable coding emerges from coactivation of climbing fibers in microbands of cerebellar purkinje neurons. ***The Journal of Neuroscience, 29*****(34), 10463.**

Paxinos, G., & Watson, C. (1998). ***The rat brain in stereotaxic coordinates.*** **San Diego: Academic Press.**

Person, A. L., & Raman, I. M. (2010). Deactivation of l-type ca current by inhibition controls LTP at excitatory synapses in the cerebellar nuclei. ***Neuron, 66*****(4), 550-9. doi:10.1016/j.neuron.2010.04.024**

Person, A. L., & Raman, I. M. (2012). Purkinje neuron synchrony elicits time-locked spiking in the cerebellar nuclei. ***Nature, 481*****(7382), 502-5. doi:10.1038/nature10732**

Phillipson, O. T. (1979). Afferent projections to the ventral tegmental area of tsai and interfascicular nucleus: A horseradish peroxidase study in the rat. ***The Journal of Comparative Neurology, 187*****(1), 117-43. doi:10.1002/cne.901870108**

Pierce, K., & Courchesne, E. (2001). Evidence for a cerebellar role in reduced exploration and stereotyped behavior in autism. ***Biological Psychiatry, 49*****(8), 655-664.**

Pologruto, T. A., Sabatini, B. L., & Svoboda, K. (2003). Scanimage: Flexible software for operating laser scanning microscopes. ***Biomedical Engineering Online, 2*****, 13. doi:10.1186/1475-925X-2-13**

Polsky, A., Mel, B. W., & Schiller, J. (2004). Computational subunits in thin dendrites of pyramidal cells. ***Nature Neuroscience, 7*****(6), 621-7. doi:10.1038/nn1253**
Pugh, J. R., & Raman, I. M. (2006). Potentiation of mossy fiber epscs in the cerebellar nuclei by NMDA receptor activation followed by postinhibitory rebound current. ***Neuron, 51*****(1), 113-23. doi:10.1016/j.neuron.2006.05.021**
Pugh, J. R., & Raman, I. M. (2008). Mechanisms of potentiation of mossy fiber epscs in the cerebellar nuclei by coincident synaptic excitation and inhibition. ***The Journal of Neuroscience : The Official Journal of the Society for Neuroscience, 28*****(42), 10549-60. doi:10.1523/JNEUROSCI.2061-08.2008**
Pugh, J. R., & Raman, I. M. (2009). Nothing can be coincidence: Synaptic inhibition and plasticity in the cerebellar nuclei. ***Trends in Neurosciences, 32*****(3), 170-7. doi:10.1016/j.tins.2008.12.001**
Racine, R. J., Wilson, D. A., Gingell, R., & Sunderland, D. (1986). Long-Term potentiation in the interpositus and vestibular nuclei in the rat. ***Experimental Brain Research. Experimentelle Hirnforschung. Expérimentation Cérébrale, 63*****(1), 158-62.**
Raman, I. M., Gustafson, A. E., & Padgett, D. (2000). Ionic currents and spontaneous firing in neurons isolated from the cerebellar nuclei. ***The Journal of Neuroscience, 20*****(24), 9004.**
Sadnicka, A., Hoffland, B. S., Bhatia, K. P., van de Warrenburg, B. P., & Edwards, M. J. (2012). The cerebellum in dystonia - help or hindrance? ***Clinical Neurophysiology : Official Journal of the International Federation of Clinical Neurophysiology, 123*****(1), 65-70. doi:10.1016/j.clinph.2011.04.027**
Schmahmann, J. D. (1998). Dysmetria of thought: Clinical consequences of cerebellar dysfunction on cognition and affect. ***Trends in Cognitive Sciences, 2*****(9), 362-71.**
Schmahmann, J. D. (2004). Disorders of the cerebellum: Ataxia, dysmetria of thought, and the cerebellar cognitive affective syndrome. ***The Journal of Neuropsychiatry and Clinical Neurosciences, 16*****(3), 367-78. doi:10.1176/appi.neuropsych.16.3.367**
Schultz, W., Montgomery, E. B., & Marini, R. (1979). Proximal limb movements in response to microstimulation of primate dentate and interpositus nuclei mediated by brain-stem structures. ***Brain : A Journal of Neurology, 102*****(1), 127-46.**
Sjöström, P. J., Rancz, E. A., Roth, A., & Häusser, M. (2008). Dendritic excitability and synaptic plasticity. ***Physiological Reviews, 88*****(2), 769-840. doi:10.1152/physrev.00016.2007**
Sobel, E. C., & Tank, D. W. (1993). Timing of odor stimulation does not alter patterning of olfactory bulb unit activity in freely breathing rats. ***Journal of Neurophysiology, 69*****(4), 1331-7.**
Soteropoulos, D. S., & Baker, S. N. (2008). Bilateral representation in the deep cerebellar nuclei. ***The Journal of Physiology, 586*****(4), 1117-36. doi:10.1113/jphysiol.2007.144220**
Steuber, V., De Schutter, E., & Jaeger, D. (2004). Passive models of neurons in the deep cerebellar nuclei: The effect of reconstruction errors. ***Neurocomputing, 58,*** **563-568.**
Stoodley, C. J., & Schmahmann, J. D. (2009). Functional topography in the human cerebellum: A meta-analysis of neuroimaging studies. ***Neuroimage, 44*****(2), 489-501. doi:10.1016/j.neuroimage.2008.08.039**
Stoodley, C. J., Valera, E. M., & Schmahmann, J. D. (2012). Functional topography of the cerebellum for motor and cognitive tasks: An fmri study. ***Neuroimage, 59*****(2), 1560-70. doi:10.1016/j.neuroimage.2011.08.065**
Strick, P. L., Dum, R. P., & Fiez, J. A. (2009). Cerebellum and nonmotor function. ***Annual Review of Neuroscience, 32,*** **413-34. doi:10.1146/annurev.neuro.31.060407.125606**

Stuart, G., & Häusser, M. (1994). Initiation and spread of sodium action potentials in cerebellar purkinje cells. ***Neuron, 13*****(3), 703-12.**
Stuart, G. J., & Sakmann, B. (1994). Active propagation of somatic action potentials into neocortical pyramidal cell dendrites. ***Nature, 367*****(6458), 69-72. doi:10.1038/367069a0**
Sugitani, M. (1979). Electrophysiological and sensory properties of the thalamic reticular neurones related to somatic sensation in rats. ***The Journal of Physiology, 290*****(2), 79-95.**
Thach, W. T., Goodkin, H. P., & Keating, J. G. (1992). The cerebellum and the adaptive coordination of movement. ***Annual Review of Neuroscience, 15*****, 403-42. doi:10.1146/annurev.ne.15.030192.002155**
Thomson, W. (1884). ON A CASE OF PISTOL-SHOT WOUND OF THE CEREBELLUM. ***The Lancet, 124*****(3183), 361-363.**
Toole, B. P. (2004). Hyaluronan: From extracellular glue to pericellular cue. ***Nature Reviews. Cancer, 4*****(7), 528-39. doi:10.1038/nrc1391**
Tsai, P. T., Hull, C., Chu, Y., Greene-Colozzi, E., Sadowski, A. R., Leech, J. M., . . . Sahin, M. (2012). Autistic-Like behaviour and cerebellar dysfunction in purkinje cell tsc1 mutant mice. ***Nature, 488*****(7413), 647-51. doi:10.1038/nature11310**
Uusisaari, M., & Knöpfel, T. (2010). Glyt2+ neurons in the lateral cerebellar nucleus. ***Cerebellum (London, England), 9*****(1), 42-55. doi:10.1007/s12311-009-0137-1**
Uusisaari, M., Obata, K., & Knöpfel, T. (2007). Morphological and electrophysiological properties of gabaergic and non-gabaergic cells in the deep cerebellar nuclei. ***Journal of Neurophysiology, 97*****(1), 901-11. doi:10.1152/jn.00974.2006**
Watabe-Uchida, M., Zhu, L., Ogawa, S. K., Vamanrao, A., & Uchida, N. (2012). Whole-Brain mapping of direct inputs to midbrain dopamine neurons. ***Neuron, 74*****(5), 858-73. doi:10.1016/j.neuron.2012.03.017**
Yang, B. Y., & Weisz, D. J. (1992). An auditory conditioned stimulus modulates unconditioned stimulus-elicited neuronal activity in the cerebellar anterior interpositus and dentate nuclei during nictitating membrane response conditioning in rabbits. ***Behavioral Neuroscience, 106*****(6), 889-99. doi:1335268**
Yu, X. J., Meng, X. K., Xu, X. X., & He, J. (2011). Individual auditory thalamic reticular neurons have large and cross-modal sources of cortical and thalamic inputs. ***Neuroscience, 193*****, 122-31. doi:10.1016/j.neuroscience.2011.07.040**
Yu, X. J., Xu, X. X., He, S., & He, J. (2009). Change detection by thalamic reticular neurons. ***Nature Neuroscience, 12*****(9), 1165-70. doi:10.1038/nn.2373**
De Zeeuw, C. I., & Berrebi, A. S. (1995). Postsynaptic targets of purkinje cell terminals in the cerebellar and vestibular nuclei of the rat. ***The European Journal of Neuroscience, 7*****(11), 2322-33.**
Zhang, W., Shin, J. H., & Linden, D. J. (2004). Persistent changes in the intrinsic excitability of rat deep cerebellar nuclear neurones induced by EPSP or IPSP bursts. ***The Journal of Physiology, 561*****(Pt 3), 703-19. doi:10.1113/jphysiol.2004.071696**
Zheng, N., & Raman, I. M. (2009). Ca currents activated by spontaneous firing and synaptic disinhibition in neurons of the cerebellar nuclei. ***The Journal of Neuroscience : The Official Journal of the Society for Neuroscience, 29*****(31), 9826-38. doi:10.1523/JNEUROSCI.2069-09.2009**
Zheng, N., & Raman, I. M. (2010). Synaptic inhibition, excitation, and plasticity in neurons of the cerebellar nuclei. ***Cerebellum (London, England), 9*****(1), 56-66. doi:10.1007/s12311-009-0140-6**